International Journal of Pharmaceutics 632 (2023) 122589

Contents lists available at ScienceDirect

International Journal of Pharmaceutics

journal homepage: www.elsevier.com/locate/ijpharm

Review

Current approaches for the recreation of cardiac ischaemic environment *in vitro*

Laura Paz-Artigas [a,b], Pilar Montero-Calle [c], Olalla Iglesias-García [c], Manuel M. Mazo [c,d], Ignacio Ochoa [a,b,e,*], Jesús Ciriza [a,b,e,*]

[a] Tissue Microenvironment (TME) Lab, Aragón Institute of Engineering Research (I3A), University of Zaragoza, 50018 Zaragoza, Spain
[b] Institute for Health Research Aragón (IIS Aragón), 50009 Zaragoza, Spain
[c] Regenerative Medicine Program, Cima Universidad de Navarra, and Instituto de Investigación Sanitaria de Navarra (IdiSNA), Pamplona, Spain
[d] Hematology and Cell Therapy, Clínica Universidad de Navarra, and Instituto de Investigación Sanitaria de Navarra (IdiSNA), Pamplona, Spain
[e] CIBER-BBN, ISCIII, Zaragoza, Spain

ARTICLE INFO

Keywords:
Cardiac ischaemia models
Heart-on-chip
Organoids
Spheroids
Scaffolds

ABSTRACT

Myocardial ischaemia is one of the leading dead causes worldwide. Although animal experiments have historically provided a wealth of information, animal models are time and money consuming, and they usually miss typical human patient's characteristics associated with ischemia prevalence, including aging and comorbidities. Generating reliable in vitro models that recapitulate the human cardiac microenvironment during an ischaemic event can boost the development of new drugs and therapeutic strategies, as well as our understanding of the underlying cellular and molecular events, helping the optimization of therapeutic approaches prior to animal and clinical testing. Although several culture systems have emerged for the recreation of cardiac physiology, mimicking the features of an ischaemic heart tissue in vitro is challenging and certain aspects of the disease process remain poorly addressed. Here, current in vitro cardiac culture systems used for modelling cardiac ischaemia, from self-aggregated organoids to scaffold-based constructs and heart-on-chip platforms are described. The advantages of these models to recreate ischaemic hallmarks such as oxygen gradients, pathological alterations of mechanical strength or fibrotic responses are highlighted. The new models represent a step forward to be considered, but unfortunately, we are far away from recapitulating all complexity of the clinical situations.

1. Modelling heart ischaemia

1.1. Myocardium characteristics

Although in its first embryonic stages the myocardium develops within a hypoxic environment (Dunwoodie, 2009), it soon turns into a high oxygen demanding tissue. The heart is one of the first organs to function and keeps on throughout an individuaĺs lifespan. It is responsible for the continuous supply of blood to the organism and does so through an efficient pumping cycle. This strenuous work comes with a strict metabolic demand: it is estimated that the heart recycles around 6 kg of ATP per day (Neely and Morgan, 1974), most of which is produced through the aerobic oxidation of fatty acids. In consequence, the myocardium has a stringent oxygen demand that is tightly tied to organ performance, and where its perturbance has acute functional effects.

The heart is a complex organ. Its function is intimately related to its 3D organization, where contractile units align to deliver force production. These units are cardiomyocytes (CMs), which are able to respond to a membrane depolarization stimulus with a series of events leading to cellular contraction (MacLeod, 2014). Although CMs are the most notorious cellular type in the heart, they are not the only component, with vascular, stromal (fibroblasts), neural and immune cells

Abbreviations: αSA, α-sarcomeric actinin; AVN, atrioventricular node; cTnT, Troponin-T; CM, cardiomyocyte; ECM, extracellular matrix; hADSC, human adipose-derived stem cell; hCF, human cardiac fibroblast; hIPSC, human induced pluripotent stem cell; HUVEC, human umbilical vein endothelial cell; IL6, interleukine 6; MI, myocardial infarction; VEGF-A, vascular endothelial growth factor A.

* Corresponding authors at: University of Zaragoza – I3A | IIS Aragón || CIBER-BBN, Campus Rio Ebro, Mariano Esquillor s/n, Edificio I+D+I, 50018 Zaragoza, Spain.

E-mail addresses: iochgar@unizar.es (I. Ochoa), jeciriza@unizar.es (J. Ciriza).

https://doi.org/10.1016/j.ijpharm.2023.122589
Received 4 October 2022; Received in revised form 14 December 2022; Accepted 4 January 2023
Available online 6 January 2023

performing crucial actions, often highly intertwined. Cardiomyocytes constitute the largest fraction by volume, but myocardial cellular proportions have been revisited, showing that in rodents, it is endothelial cells the most abundant cell type (Pinto et al., 2016). This is especially notorious upon histological inspection, with each large CM in close contact with several vessels (capillaries), a structure that is well conserved between species, including humans. However, the issue remains controversial, further complicated by differences in abundance depending on the anatomical location (Bergmann et al., 2015). Needless to say, all cell types are essential for the correct function of the organ. Endothelial cells, lining the inner surface of blood vessels, regulate the trafficking of nutrients to the extracellular space. They have proven instrumental in key events such as tissue hypertrophy (Gogiraju et al., 2019) or post-ischemia remodelling (Segers et al., 2018). Cardiac fibroblasts are responsible for extracellular matrix (ECM) homeostasis in the tissue. Under certain pathological stimuli, such as ischemia, inflammation or persistent neurohormonal activation, these cells can differentiate into the pro-fibrotic myofibroblasts (reviewed in (Tallquist and Molkentin, 2017)). Though important in the healing process post-injury, this phenotype often fails to disappear and produces an excessive collagen deposition, leading to a functional impairment. Recently, this cell type has been subject to intense research, highlighting the heterogeneity of a previously thought as homogeneous cell type and their role in controlling cardiac function (Chou et al., 2022; Ruiz-Villalba et al., 2020). Similarly, immune cells, believed in the past to play a policing/cleaner role in the organ, are starting to reveal themselves as important modulators of CM functionality, as shown for the electrical coupling of macrophages with cardiac cells in the atrioventricular node (Hulsmans et al., 2017).

The last component of the tissue that merits mention is the ECM. The ECM is a network of glycoproteins found extracellularly, whose main component in the heart are collagens (accounting for 2–5 % of the organ dry weight). These molecules are synthesised by cardiac cells and are not only responsible for tissue organisation, but also for its mechanical properties, with for example collagen being a great contributor to myocardial tensile properties (Fomovsky et al., 2010). Of the many collagen subtypes, the most abundant are types I and III, whose balance is crucial for the said tensile properties, and type IV, found in the basement membrane and in intimate contact with cells. Other important components are elastin (especially in large vessels and valves), fibronectin and laminin.

Cardiac cells and ECM are all arranged in a 3D structure that is very specific of the organ function and can be both altered in disease or its alterations being the cause of disease (Eghbali and Weber, 1990). In cardiac morphogenesis, the different components of the organ (including chambers, valves, outflow and inflow tracts or the coronary arteries and veins, amongst others) arise and are given their specific anatomical location, responsible for the adequate unidirectional flow of blood. This 3D structure results in a contraction-torsion movement, but the specifics of the 3D architecture are still a matter of debate, with the myocardial band model (Buckberg, 2002; Buckberg et al., 2018) and the mesh model (MacIver et al., 2018b, 2018a) as the most advanced explanations. In any case, this 3D organisation not only stems from the relative cellular arrangement, but also from the disposition of the cardiac extracellular matrix (ECM).

All in all, as mentioned, the above players contribute to the proper functionality of the heart. In consequence, their alteration can lead to disease. Although cardiac disease is a broad term encompassing from congenital illnesses to acquired conditions, cardiac ischemia is of special relevance due to its impact, being the first single cause of death worldwide (Roth et al., 2020).

1.2. Cardiac ischaemia

The most common form of myocardial ischemia occurs secondary to a thrombotic event, where the rupture of an atherosclerotic plaque in a coronary vessel leads to its blockage. Depending on the affected vessel, ischemia will affect different regions in the myocardium (Frangogiannis, 2015), which is thus bereft of irrigation. Given the stringent metabolic needs of CMs, this ischemia leads to rapid pathological changes. Within minutes, CMs start developing the first signs of necropsy, including mitochondrial swelling and sarcomeric disarray. If blood flow is not speedily restored through interventions such as reperfusion, CMs soon will enter a no-return path towards death. Several cell death mechanisms have been stablished as contributors to CM death upon ischemia (Davidson et al., 2020). But, blood reperfusion, although necessary to limit ischemic damage, also causes microvasculature damage (Caccioppo et al., 2019), oxygen reactive species (ROS) concentration imbalance (Raedschelders et al., 2012), altered mitochondrial permeability and membrane potential. Moreover, in blood reperfusion CMs show hypercontracture, due to ATP production recovery in the overloaded presence of Ca^{2+} accumulated during ischemia (Inserte et al., 2009). While the redox balance is complex and may also have a cardioprotective role (Pagliaro and Penna, 2015), overall reperfusion effects enhance cell death pathways initiated during ischemia, resulting in the ischaemia/reperfusion (I/R) injury.

The process after a myocardial ischemia is traditionally divided in 3 sequential yet overlapping phases (Mazo et al., 2010). Firstly, there is a massive influx of inflammatory cells, first granulocytes, then macrophages, which will clear the cell debris and help maintain the integrity of the cardiac wall. In a second stage, termed proliferative phase, the inflammatory infiltrate is progressively cleared away, whilst fibroblasts are recruited to the injured site. The presence of inflammatory and profibrotic signals, added to the mechanical stress, trigger the transition of these cells to a myofibroblasts phenotype. Myofibroblasts deposit a collagenous scar, akin to the healing of a skin cut. However, in stark contrast, myofibroblasts in the heart do not disappear, and continue depositing ECM in what is called the healing phase. The chronification of this collagen deposition leads to the appearance of a hyper-stiff scar, with an increased content of collagen type III.

Under this situation, the organ will contain less CMs to perform its function, effectively diminishing its pumping capacity. Added to this, the non-ischemic area is also impacted. For example, the collagen scar renders a significantly stiffened tissue, against which the remaining contractile CMs must function, also leading to an alteration of the normal cardiac 3D architecture. The consequence is a further decrease of the efficiency of contraction. This pathological situation soon becomes chronic, leading to a maladaptive remodelling of the tissue (Frantz et al., 2022), further functional decline, and the final dichotomy of transplantation versus death.

1.3. Evolution of experimental models of cardiac ischemia

Studying human cardiac ischemia has traditionally relied in 2 types of models: 2D in vitro cell culture and animals. In vitro, control of pO_2 can be easily achieved in cell culture incubators through the controlled infusion of an inert gas such as N_2. However, a sharp control of hypoxia can be challenging, as opening the incubator, or taking cells out to change medium will immediately increase oxygen levels to normoxia (reviewed in (Pavlacky and Polak, 2020)). Several commercial devices have been developed to address this issue, but in general these are not widespread. Two-dimensional models have heavily relied on the use of rodent cells, especially neonatal rat ventricular CMs. These cells can be readily isolated from rat pup hearts using mechanical and enzymatic disaggregation (Pereira et al., 2021). They are functional and can be maintained in cultured for several days. However, even if almost pure at isolation, presence of contaminating cardiac cells, fundamentally fibroblasts, will eventually overtake non-dividing CMs, rendering long-term experiments not viable. Also, the neonatal nature of these cells makes them inherently immature, with lack of salient features such as *T*-tubules or aligned sarcomeres (Sheehy et al., 2017). Adult CMs can also be isolated from rodents using techniques such as Langendorff perfusion

(Li et al., 2020). These cells, though relevant, are scarce and show a culture lifespan of days, as they soon enter an artificial dedifferentiation process. Other cellular models include cell lines such as mouse HL-1 and rat H9C2 cells. Although thanks to models based on animal cell lines, easy to handle in the lab, have helped to clarify aspects of cardiac cell biology, differences to human cardiac cells in terms of structure (presence of sarcomeres, CXs, amongst others) and function (such as low conduction velocity or irregular beating) may reduce the predictive power of these models.

Cardiac ischemia is induced in animal models through surgical ligation of a coronary artery (Mazo et al., 2010), though cryoinjury has sometimes been used as a simple surrogate (von Bibra et al., 2022). However, it presents evident differences from ischemia, as the tissue is scarred, and ischemia develops secondary. In consequence it is rarely employed. Ligation-based models are more widespread but technically demanding, as reproducibility of the extent of ischemia (and thus of the functional impairment) highly depends on the experience of the surgeon. Although still artificial, ligation models recapitulate the different phases of post-ischemia healing and remodelling, including the cellular phenotypes modulation and structural impact (Mazo et al., 2010). Broadly speaking, ligation-based models of cardiac ischemia can be mainly divided between those producing a chronic ischemia, and those where the ligation is withdrawn, mimicking reperfusion interventions in patients, and termed "ischemia/reperfusion". This model is thought to be more translationally relevant, as most patients are in fact reperfused if deemed safe.

The purpose of both 2D in vitro and animal models is to recapitulate as faithfully as possible the characteristics of the pathological process. However, their animal nature constitutes an unbridgeable gap. On the other side, human primary CMs are very scarce, as human cardiac tissue is not readily available. In fact, most human myocardial samples are obtained from already diseased individuals, as for example a recipient́s heart after a transplant, making them unsuitable unless the specific disease of the patient is being studied. In 1998, James Thomson derived the first human embryonic stem cells (Thomson et al., 1998). These cells soon proved capable of giving rise to human CMs (Laflamme et al., 2007). Few years later, the derivation of the first human induced pluripotent stem cells (hiPSCs) and the generation of CMs with increasingly refined differentiation protocols, opened the path to the obtaining of human cardiac cells beyond CMs (Nakagawa et al., 2007; Yu et al., 2007; Zwi et al., 2009), without ethical constrains and in virtually unlimited supply. These cells, though human and thus more relevant than previous in vitro models, still faced limitations such as their immature nature (Karbassi et al., n.d.), being more like embryonic human CMs than their adult counterpart. This is a significant issue given that cardiac ischemia usually affects adults.

In addition to these, it has been increasingly evident that 2D, though informative, is not representative of the in vivo situation. Organs and tissues are 3D, and this, as already mentioned in prior sections, has crucial implications for myocardial function and, for the development of accurate models, including of cardiac ischemia. Therefore, in the last three decades, efforts have been made to recreate more straightforward cell microenvironment than classical 2D cultures. Novel approaches aim to recapitulate in vivo cellular diversity of human tissues, its precise architecture, and various cellular stimuli (e.g., mechanical or electrical). These new models represent an intermediate step between classical in vitro cultures and experimental animals, reproducing closer physiological conditions than classical 2D in vitro cultures, while entailing lower ethical concerns, time, and money expenses than animal models. Although, new in vitro approaches cannot fully recreate the complex response of the entire body during disease, they offer wide possibilities for in situ monitoring of human cellular response, helping to unravel specific cellular mechanisms and responses to drugs or experimental treatments.

2. Scaffold-free models: Cardiac spheroids and organoids

2.1. Physiological heart spheroids

The ability of most cells to self-assemble has been largely used for generating 3D scaffold-free aggregates, known as spheroids or organoids. This nomenclature has been quite confusing in the literature. Since there is no widespread consensus on the differences between both terms, here we will refer to spheroids as aggregates of differentiated cells, and organoids as aggregates of stem cells differentiated after aggregation. Spheroids and organoids are easy and quick to form and constitute a closer model of the human tissue's physiological 3D microenvironments than monolayer cultures. They reproduce cellular network connections and diffusion movements of nutrients or drugs. Several tissues, such as brain (Privat-Maldonado et al., 2018), liver (Leedale et al., 2020) or kidney (Kang et al., 2019), have been modelled by culturing cells as hanging drops or in U-shaped, low-attachment wells, which favours cell-to-cell connections and aggregate formation.

First attempts to recreate myocardium using spheroids were based on the culture of neonatal rat and mouse CMs (Kelm et al., 2006, 2004), since primary adult cells lose their functionality after few days in culture (Louch et al., 2011). The development of CM differentiation techniques of hiPSC, though, as mentioned, usually immature in phenotype, led to the generation of the first human cardiac spheroids (Beauchamp et al., 2015). In fact, 3D culture has proved to enhance the maturity of CM derived from hiPSC (hiPSC-CM) (Correia et al., 2018). Moreover, organoids allow the coculture of the different cell types that constitute a certain tissue and their self-organization into a physiological architecture. Thus, hiPSC-CM have been cultured with cardiac fibroblasts, endothelial cells, or mesenchymal cells in organoids, more closely mimicking the complexity of myocardial structure and functionality (Lee et al., 2019; Yang et al., 2019), with cardiac spheroids and organoids showing intrinsic contractile activity (Desroches et al., 2012; Polonchuk et al., 2017). In fact, they have been electrically or mechanically stimulated to enhance contraction and maturation of CMs (LaBarge et al., 2019; Stevens et al., 2009; Tan et al., 2015).

Main methods to monitor spheroids and organoids include cytokine and factor release quantification, characterization of oxygen consumption rate and metabolic pathways, Transmission Electron Microscopy (TEM), architecture and cell phenotype determination by immunofluorescence, transcriptomic analysis or optical tracking of calcium and contraction (Archer et al., 2018; Beauchamp et al., 2015; Giacomelli et al., 2020; Lewis-Israeli et al., 2021). Nevertheless, self-assembly does not achieve a functional 3D architecture similar to the natural myocardium, such as cell alignment, and does not allow direct contraction force measurement. Therefore, methods to spatially organize and electromechanically integrate spheroids into larger functional structures may overcome these spheroid pitfalls (Kim et al., 2018).

2.2. Modelling cardiac ischaemia via spheroids

In vivo cardiac infarction injury is spatially characterized by a gradient of gravity from the seriously damaged centre of the infarcted area to a remote zone, where the effects of the blood flow arrest are less aggressive. Despite spheroids intrinsic capacity to reproduce nutrients and oxygen gradients, few attempts have been done to recreate myocardial ischaemia via spheroid or organoid modelling. In standard normoxic conditions (21 % O_2), cardiac spheroids with radius smaller than 150 μm (oxygen diffusion rate in cardiac engineered tissue (Brown et al., 2007)) maintain good viability throughout the spheroid (Archer et al., 2018; Desroches et al., 2012). However, when those cardiac spheroids are subjected to diverse chemical or biological stimulus, they can mimic different ischaemic events (Table 1).

Cardiomyocyte damage during myocardial infarction (MI) is initially caused by the limitation of oxygen and nutrients availability, but exacerbated after reperfusion. Thus, I/R injury can be mimicked in

Table 1
Cardiac spheroid models assessing different features of myocardial ischaemic injury.

Spheroid generation	Cell types	Ischaemic stimulus	Ischaemic hallmark recreated	Ref.
1500 cells/spheroid AggreWell400Ex plates, followed by orbital suspension culture Seeded at day 7 of CM differentiation and cultured for 18 days (to reach complete differentiation and maturation) ≈260 μm diameter	hiPSC-CMs	5 h of ischaemia: Nutrient reduction (Ischaemic Mimetic Solution) less than 0.4 % O_2 16 h of reperfusion: control conditions restoration	Apoptosis Lacunae at spheroid core Disrupted sarcomere myofilaments and Z band organization Mitochondria alterations Increase in inflammatory, angiogenetic and migration-related secretions	(Sebastião et al., 2020)
4000 cells/spheroid agarose micromolds 4 days' incubation for self-assembly ≈150 μm diameter	hiPSC-CMs hCFs HUVECs hADSCs (ratio 7:4:2:1)	6 h of ischaemia: Nutrient reduction (serum free, low glucose medium) 1 % O_2	Increased secretion of IL6 Increased secretion of VEGF-A	(Richards et al., 2017)
4000 cells/spheroid agarose micromolds 4 days' incubation for self-assembly ≈150 μm diameter	hiPSC-CMs hCFs HUVECs hADSCs (ratio 7:4:2:1)	10 days of ischaemia: 10 % O_2 1 μM noradrenaline	Reduced-oxygen environment Anaerobic metabolism Pathological fibrosis Inner apoptosis Arrhythmic calcium handling and contractile activity Higher susceptibility to cardiotoxic drugs Decrease of MI effects after anti-MI drug treatment	(Richards et al., 2020b)

cardiac organoids of hiPSC-CMs matured after organoid formation by deprivation of nutrient and oxygen for 5 h, followed by standard conditions restoration for 16 h (Sebastião et al., 2020). The I/R protocol results in apoptosis and cell death after ischaemia, which is exacerbated during reperfusion, with no significant change in organoids diameter. In concordance with these results, immunofluorescence from organoids cryosections shows lacunae in the core of organoids subjected to I/R simulation. hiPSC-CMs maintain the expression of the cardiac markers Troponin-T (cTnT) and α-sarcomeric actinin (αSA), but present disrupted sarcomere myofilaments and Z-band organization, and higher density of mitochondria with disorganized cristae and membrane rupture. I/R simulation also increases organoid expression of inflammation, angiogenesis and migration related molecules. In fact, conditioned media of organoids subjected to I/R increases the angiogenetic potential of human umbilical vein endothelial cells (HUVEC) and causes human cardiac progenitor cells to express genes related to migration, proliferation, paracrine signalling, and stress response.

While the aforementioned model recapitulates relevant responses of CM to I/R injury, several additional processes triggered by myocardial ischaemia depend on other cardiac cell types, like angiogenesis or fibrosis, and cannot be simulated by a monoculture of hiPSC-CMs. Thus, hiPSC-CMs cocultured in spheroids with human cardiac fibroblasts (hCFs), human adipose-derived stem cells (hADSCs), and human umbilical vein endothelial cells (HUVECs) (Richards et al., 2017) offer a more complex cardiac model. Spheroids with a cell ratio corresponding to that of the developing myocardium result in better development of hiPSC-CMs structure and functionality than those built under an adult-like ratio (i.e., higher proportion of hCFs) 10 days after seeding. Spheroids are then subjected to 6 h of nutrient and oxygen reduction, simulating ischaemia, with no reperfusion afterwards. Ischaemia causes an increase in interleukine 6 (IL6) and vascular endothelial growth factor A (VEGF-A) expression, both characteristic of an ischaemic heart event. IL6 secretion increase is attributed to the presence of hCFs, since only-hCFs spheroids show the highest levels of IL6 gene expression, confirming the importance of co-culture for a proper modelling. Although all single-cell-type spheroids show VEGF-A increase, hiPSC-CMs spheroids and hCFs spheroids present the highest increase, suggesting a leading role of CMs and hCFs in ischaemic VEGF signalling.

This cardiac spheroid model has been used to simulate post-myocardial infarction (post-MI) tissue by truly recreating an oxygen gradient within the spheroid (Richards et al., 2020a). Previous studies have worked with oxygen pressures below 1 %, which led to homogenous hypoxia throughout the whole spheroid. Conversely, these cardiac spheroids are incubated for 10 days with a partially reduced oxygen concentration (10 % O_2), seeking for a highly hypoxic core and a more functional edge (Fig. 1). Damaged myocardial tissue in vivo usually presents a reduced ability to pump blood to the body, which triggers nervous system adrenergic stimulation with noradrenaline. This positive feedback cannot be fully compensated by the damaged tissue and may lead to major heart dysfunction (Frangogiannis, 2015). To recreate this compensatory demand stimulus, spheroids were treated with 1uM noradrenaline in addition to the oxygen reduction. After 10 days, spheroids showed a shift towards anaerobic metabolism, pathological fibrosis (which is absent in single-cell-type hiPSC-CM spheroids), as well as arrhythmic calcium handling and contractile activity, therefore recapitulating major aspects of in vivo ischaemic myocardium. Notably, spheroids showed a NADH autofluorescence gradient, indicating reduced-oxygen environment in the spheroid centre, that correlates with the presence of apoptotic cells in the same area Fibrotic remodelling caused an increase in vimentin organization towards the edge of the spheroids and led to higher spheroid stiffness. Spheroids produced with hiPSC-CMs from a different donor showed similar results, indicating the robust translation of this ischaemia model. Further confirmation of the post-MI spheroid suitability as a model in drug research was assessed by testing the cardiotoxic effect from doxorubicin (a cardiotoxic anticancer medication) and the potential protective effect of JQ1 (an anti-fibrotic drug) for heart failure. Spheroids subjected to the MI protocol showed higher susceptibility to the toxic effects of doxorubicin than control spheroids, and incubation with JQ1 through the whole MI protocol duration resulted in significant reduction of the ischaemia effects. These results highlight the potential benefits of this model for preclinical drug testing.

Several aspects of myocardial ischaemic injury have been reproduced in different cardiac spheroid and organoids models so far, with encouraging results. However, a model that fully combines mature and cell-diverse myocardium with true ischaemic oxygen and nutrient gradients, along with reperfusion effects and adrenergic stimulation must still be implemented. Moreover, spheroids inherent features prevent cardiac cell alignment, fundamental for enhanced cardiac contractile functionality, and implementation of mechanical stimulation. Real time monitoring of gas and nutrients mass transport and cell response inside spheroids can also be an important drawback of cardiac spheroids models.

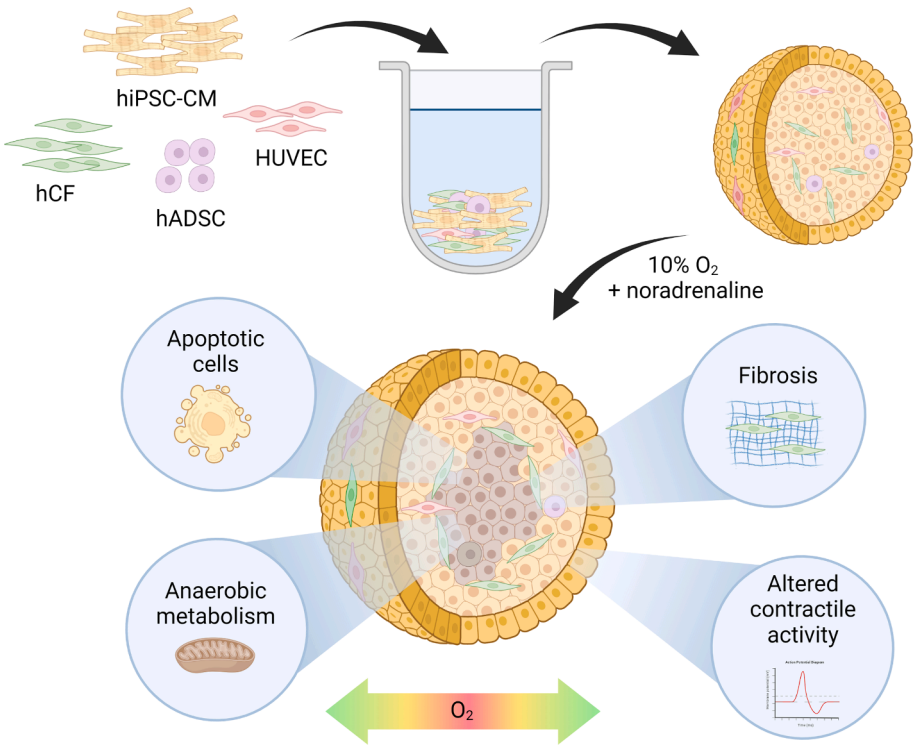

Fig. 1. Recreation of an ischaemic oxygen gradient within a cardiac spheroid. Spheroids are generated by coculture of hiPSC-CMs with hCFs, HUVECs and hADSCs; and then subjected to 10 days of oxygen partial deprivation and noradrenaline stimulation. An oxygen gradient is generated within the spheroid, with a highly hypoxic core, leading to apoptosis, anaerobic metabolism switch, tissue fibrotic remodelling and alterations in calcium handling and contractile activity. Created with BioRender.com.

3. Engineered cardiac tissues

3.1. Biomaterials for the recreation of myocardial tissue architecture

The use of biomaterials that mimic the extracellular matrix (ECM) for cell culture allows a high control of 3D construct architecture, including microtissue shape, cell alignment or density, which is not achievable by self-aggregation of cells (Joshi et al., 2018a; Lee et al., 2008). Biomaterials meant to recreate cardiac ECM must provide cells with a microenvironment akin to the native cardiac tissue, mimicking anisotropy, elasticity, mechanical strength and electromechanical coupling (Bursac et al., 2002; Deitch et al., 2012; Herron et al., 2016; Wang et al., 2011). To meet these features, different materials may be chosen and modified, with regards to their biocompatibility, porosity, fibrillary density, electrical conductivity, stiffness, anisotropy, or degradation kinetics.

The biomaterials that most accurately reproduce the complex architecture and features from cardiac tissue are decellularized ECMs. Cells from native cardiac tissues are removed via enzymatic, chemical or physical procedures, leaving a fibrillary network of macromolecules that maintain intact the main features of the original native ECM (Heath, 2019) and can be used as a scaffold for new cell seeding. While scaffolds from decellularized human myocardium would ensure the biomimetic environment for human cells, source availability is substantially limited (Guyette et al., 2016). Thus, extensive work has been done to optimize decellularization protocols for animal sources, mainly pig hearts, given their large size and high similarity with the human heart (Hodgson et al., 2017). Plant-derived biomaterials, such as decellularized cellulose network, have also been investigated for the reproduction of scaffolds for tissue engineering, avoiding immunogenicity incompatibilities (Fontana et al., 2017). However, independently of the original source, decellularization processes are long and complex and a complete cell removal usually compromises ECM integrity (Liao et al., 2020; Mendibil et al., 2020).

De novo generation of 3D scaffolds by polymerization of natural or synthetic polymers into biocompatible hydrogels represents a simplified and widespread approach to mimic the ECM. Cells are mixed with the polymer liquid solution prior to polymerization, obtaining homogeneous seeding through the scaffold, whose geometry can be easily tuned using different casting molds (Jackman et al., 2016; Li et al., 2018). Hydrogels present good diffusion properties, and high permeability for oxygen, nutrients, and other water-soluble metabolites (Saludas et al., 2017). To meet the optimal scaffold properties for cardiac tissue engineering, a wide range of hydrogel materials can be used. Natural polymers, such as collagen or fibrin, show high biocompatibility and biodegradability and can mimic components of the ECM. Collagens I and III are the most abundant structural proteins of the mammalian myocardium ECM (Frangogiannis, 2017) and have been used for cardiac tissue engineering (Ruan et al., 2016; Zhang et al., 2017), even though collagen scaffolds are stiffer than other hydrogels, do not easily remodel to allow high cell density and interconnectivity, and do not stimulate endogenous matrix secretion by cardiac fibroblasts (Pomeroy et al., 2020). Fibrin overcomes these issues and is recently gaining ground over collagen (Jackman et al., 2016; Matveeva et al., 2020). However, fibrin presents significant batch-to-batch variability, low mechanical strength and a fast degradation rate (Khodabukus and Baar, 2009; Matveeva et al., 2020). Chemical modification of these proteins, or combination with basal lamina proteins, such as the commercial mixture Matrigel (Li et al., 2018), can improve hydrogels performance as cardiac scaffolds. Other natural polymers such as gelatin (Gaetani et al., 2015; Navaei et al., 2016), chitosan (Jiang et al., 2019) and hyaluronic acid (HA) (Gaetani et al., 2015) have also been used for cardiac scaffold production. Synthetic polymers, in turn, offer an extended versatility for different chemical and physical needs, but must ensure high biocompatibility and cardiac functionality. Hydrogels of poly(ethylene glycol) (PEG) (Basara et al., 2022) and fibrous mesh generated from poly(DL-lactic-*co*-glycolic acid) (PLGA) (Chen et al., 2015), poly(glycerol sebacate) (PGS) (Ravichandran et al., 2013), or poly 3-hydroxybutyrate (PHB) (Cristallini et al., 2014) are examples of synthetic polymers that have been used to recreate cardiac scaffolds.

Recently developed techniques for micro- and nanofabrication have been applied to scaffold production, patterning biomaterials, including the aforementioned polymers, with precise control of the chemistry, topography, elasticity, and conductivity of the resulting scaffold. The

electrospinning technique, consisting of the application of electrostatic forces to a polymer solution to obtain nanofibers that can be deposited as a nanofibrous scaffold, has recently incorporated the use of native ECM proteins to generate engineered heart tissues (EHTs) (Joshi et al., 2018b). Bioprinting (i.e., layer-by-layer deposition of biomaterials called bioinks with a defined pattern) has also been applied to cardiac scaffold fabrication with promising results, since it allows complex biomaterial ink composition, high spatial resolution, and the possibility to add cells to the ink prior to scaffold formation (Maiullari et al., 2018). However, nanofabrication technologies still need to be optimized to overcome present limitations, such as low porosity, difficulties in scaling-up and in efficient incorporation of various ECM proteins (Pomeroy et al., 2020; Zhao et al., 2015).

3.2. *Modelling cardiac ischaemia via scaffolds*

Cardiac cell culture within scaffolds allows the generation of cardiac constructs with defined shapes, dimensions, and cellular densities, advantageous to model ischaemia. Disk-shape scaffolds of defined thickness (1.5–2 mm) and high diameter/thickness ratio, loaded with different concentrations of neonatal rat ventricular CMs, were used to characterize the effects of oxygen and nutrient gradients in one

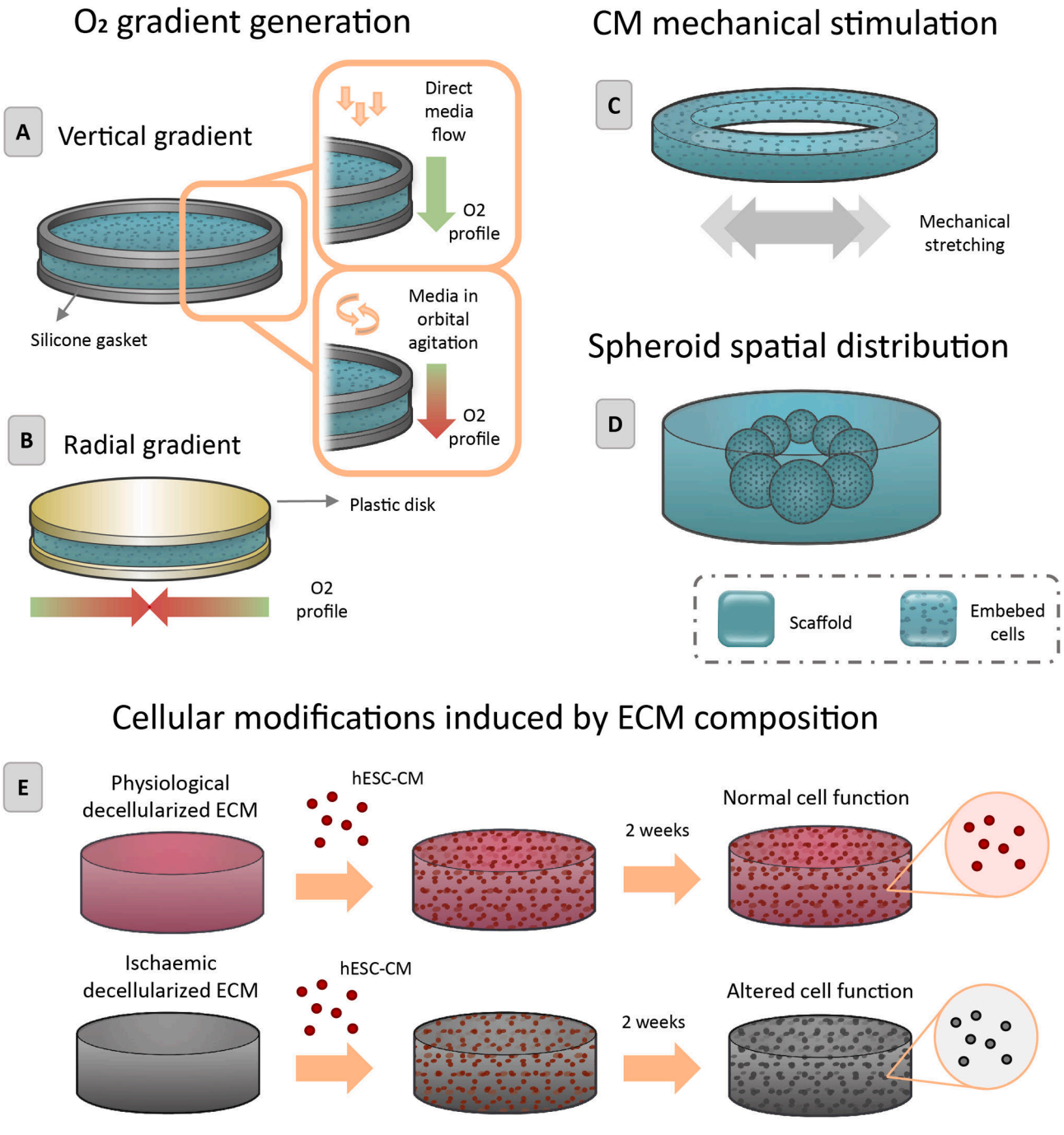

Fig. 2. Application of scaffolds in 3D cardiac models of ischaemia. Cell culture inside scaffolds allows recreation of linear (A) or radial (B) oxygen gradients. Ring-shape scaffolds (C) enable the application of mechanical stretching stimulation for CM maturation prior to ischemia induction. Scaffolds can also be used as molds (D) for the spatial distribution of "healthy" and "injured" cardiac spheroids. E) hESC-CMs suffer functional alterations after seeded within decellularized ECM (Extracellular matrix) from ischaemic heart human samples.

dimension (through the disk thickness line) (Carrier et al., 2002; Radisic et al., 2006, 2004). Cell-loaded polyglycolic acid (PGA) (Carrier et al., 2002) or collagen (Radisic et al., 2006, 2004) disks were sandwiched and sealed between two silicone gaskets, leaving an exposed area of 45–85 % of their diameter. The system was cultured for 7–16 days in spinner flasks, to guarantee a homogeneous distribution of medium around the construct, as compared to disks subjected to direct laminar medium flow (Fig. 2A). Thus, a lower pH and pO_2 was quantified at the disk surface in constructs cultured in spinner flasks than in constructs under flow regime, while pCO_2 was higher (Carrier et al., 2002). Lack of flow is translated into inhomogeneous distribution of cells, with viable cells concentrated within the outer region, suggesting a depth-dependent decrease in oxygen and nutrient availability inside the scaffold. Elongated cells expressing the sarcomeric protein α-actin with differentiated sarcomere ultrastructure located no further than 300 μm from the surface. Cell damage and death, assessed by lactate deshydrogenase (LDH) levels, were significantly higher in non-flow than in flow conditions. Furthermore, CMs isolated from constructs cultured in orbitally mixed dishes arrested at G2/M phase, apparently unable to complete the cell cycle, drifting to anaerobic metabolism, showed by the increase of the molar ratio of lactate produced/glucose consumed (L/G) (Radisic et al., 2004). Both spontaneous and electrical stimulation-related synchronous contractions were also observed in constructs, with an arrhythmic contraction pattern under flow absence. Oxygen concentration within the construct, quantified by microelectrodes, exhibited a linear decrease along the centre line, from the top construct surface to the bottom. Combination of cellular density, viability and oxygen concentration distribution data show that live cell density decreases exponentially with the decrease in oxygen concentration. Interestingly, when live cell density data are fitted to an exponential *in silico* model, oxygen concentration prediction decreased linearly, as expected. However, it is underestimated at low cell densities (under 1,000 mm depth), fitting more accurately by modifying the values of Michaelis-Menten equation parameters used to describe oxygen consumption kinetics. These results suggest that the effects of oxygen gradients in cellular distribution are dependent on cell respiration rate (Radisic et al., 2006).

Disk-shaped scaffolds can also be used to generate radial gradients of oxygen (Brown et al., 2007). In this approach, neonatal rat ventricular CMs are resuspended in a collagen-Matrigel mixture, gelled between two circular plastic disks (Fig. 2B) and cultivated in standard well plates. The plastic disks limit the medium-hydrogel interphase to the external perimeter surface of the disk, with radial diffusion rates dominating cell access to oxygen and nutrients. A wide range of experimental conditions have been tested with this approach, including variations in construct diameter (4, 6 and 7.2 mm), cell density (5, 10 and 15 x10^6cells/mL), oxygen concentration in the medium (0, 10, 20, 70 %), time of culture (0.5, 4, 18 and 36 h) and presence of metabolic inhibitors (2-deoxy-glucose and potassium cyanide). Distance from the hydrogel radial surface to the front line of hypoxic cells allows the development of a mathematical model of oxygen diffusion, whose oxygen profiles prediction correlates well with experimental data. However, although the recreation of oxygen gradients and its correlation with viable cell density has been assessed, other media component gradients, such as glucose, could enhance the relevance of this kind of 3D cardiac models. Moreover, the combination of these construct designs with the coculture of human cardiac cells like hiPSC-CM and hCF might increase their biomimicry.

The application of scaffolds to generate a wide range of cardiac construct shapes is not restricted to gradient recreation. Neonatal rat cardiac cells (50 % CMs, 50 % non-myocytes) seeded into collagen-Matrigel ring-shaped hydrogels (Fig. 2C), show irregular contractions 5 days after seeding, becoming synchronous and regular after 7 days of mechanical stretching, prior to ischaemia induction (Katare et al., 2010). Electron microscopy demonstrates the presence of developed adult CMs with normally arranged sarcomeres. In fact, mechanical stretching results in upregulation of connexin 43 and α-sarcomeric actin. Moreover, functional adult-like EHTs subjected to 6 h of hypoxia by culturing with 1 % O_2, followed by 12 h of reoxygenation, result in the downregulation of the cell survival regulators Akt and Bcl-2, dephosphorylation of gap junctional protein connexin 43 and loss of normal conduction across the EHT. Interestingly, preventive treatment with the pro-survival agents cyclosporin or acetylcholine prior to hypoxia reduces damage to EHTs, showing the potential of the model in drug research, even though animal cells may always entail differences in their response from human cells.

Mechanical stretching of ring-shaped collagen hydrogels has also been used for enhancing human cardiac cells functionality differentiated from human embryonic stem cells (hESCs) (Voges et al., 2017). After 5 days of static incubation followed by 7 days of mechanical stretching, human EHT form functional sarcomere units that display physiological inotropic responses to calcium. However, CMs-stromal cells ratio is comparable to that of the fetal/neonatal heart, and sarcomeric structures are indicative of immature CMs. In fact, cellular response to injury mimics neonatal rather than adult myocardium. To recreate a spatially focalized MI damage, the model is subjected to cryoinjury by application of a small dry-ice probe. Cryoinjury results in localized cell death, but CM cell size and fibronectin protein expression reveal no hypertrophy or fibrosis, hallmarks of adult reparative response to myocardial ischaemia in humans, and regenerating injured region at day 14, with recovered contractile forces. This functional recuperation is dependent of CM proliferation since blocking with mitomycin C prevents recovery of contraction force. Interestingly, addition of human monocytes does not upregulate proliferative response of immature CM, consistent with an angiogenic rather than a CM proliferative role of monocytes in vivo (Aurora et al., 2014). However, although this is a promising model of human neonatal myocardium, its prediction power for developing therapeutic strategies against MI is reduced, since ischaemic injury in vivo is more common in adult myocardium, which largely loses CM regenerative potential, rendering post-MI recovery tougher than in neonatal myocardium (Porrello et al., 2013).

Hydrogels have also been used as supporting molds for the spatial distribution of spheroids (Fig. 2D). A model of localized cardiac ischaemia based on the generation of a ring composed of 8 spheroids with different CM:CF rate composition embedded within a hyaluronic acid hydrogel allows to mimic electrophysiological properties of a heart chamber, including the possibility of re-entrant arrhythmias (Mastikhina et al., 2021). Since pathological fibrosis is one of the main features of adult cardiac response to ischaemic injury, spheroids with high proportion of hCF (1:4, hiPSC-CM to hCF) can recreate a damaged area, while spheroids with high proportion of hiPSC-CM (4:1, hiPSC-CM to hCF) reproduce a healthy tissue. Thus, 8 healthy spheroids printed within hydrogels can form a control ring-shape microtissue, while rings with 6–7 healthy spheroids and 1–2 “damaged” spheroids serve as a model of MI. A low polymer concentration (3 wt%) allows high cell viability 24 h after spheroids printing, reaching fusion into a microtissue ring 4 days after culture. Connexin-43 staining shows gap-junction formation in healthy regions of the microtissues but not in scarred regions. Moreover, healthy microtissues show synchronized calcium activation propagation across the entire ring, indicating functional electrical coupling between fused spheroids, while injured microtissues show wave-like propagation. Activation delay increases in microtissues containing two scarred spheroids (at opposing ends of the ring) compared to single scar. This model can recreate organotypic cell densities, supports high levels of CM-CM contact, analogous to healthy cardiac tissue, and allows the study of border zone interactions, but it fails to reproduce the anisotropic tissue alignment present in mature myocardium, and the CM damage caused by O_2 and nutrient deprivation during an ischaemic event. Damaged microtissues treatment with miRNAs for stimulating CM proliferation and cardiac repair resulted in tissue remodelling and significantly reduced activation delay, showing the model potential for the testing of therapeutic avenues.

The relevance of scaffolds for microenvironment recreation has been recently demonstrated by the differential response of CMs derived from human embryonic stem cells (hESC-CM) cultured in decellularized ECM (Fig. 2E) from either healthy or ischaemic failing human heart samples (Zhao et al., 2022). Constructs from ischaemic samples show altered contractile activity, with increased expression of α-actinin, and reduced troponin organization in hESC-CMs seeded within ischaemic ECM compared to healthy ECM, with also increased vimentin^{+} non-myocyte population in ischaemic ECM-based constructs. The observed expression is consistent with data from whole myocardium tissue proteomics of normal and ischaemic heart samples, demonstrating the importance of mimicking human myocardial ECM in cardiac ischaemia models, and how these models can be used in future personalized medicine.

Although scaffolds offer a wide range of approaches for controlling spatial cell distribution, allowing the investigation of gradients and recreating localized myocardial ischaemic injuries (Table 2), to date, O_2 gradients have only been tested on monocultures of animal CM, whose response may differ from human CM and cannot recreate hallmarks of in

Table 2
Myocardial infarction modelling via scaffolds.

Cardiac construct	Scaffold	Cell types	Ischaemic stimulus	Ischaemic hallmark recreated	Ref.
Disk sandwiched between two silicon gaskets Disk thickness: 2 mm Disk diameter: 11 mm Exposed area: 9.5 mm	Polyglycolic acid (PGA)	Neonatal rat ventricular CMs	10 days of ischaemia:Gradient of medium penetration within the disk depth in spinner flask culture (compared to uniform media perfusion through the scaffold)	Low pH and pO_2 High pCO_2 Anaerobic metabolism Spatial gradient of ischaemic effects Cells shrinkage Disorganized sarcomeres Loss of cell junctional complexes Less dense cytoplasm with fewer recognizable organelles	(Carrier et al., 2002)
Disk sandwiched between two silicon gaskets Cell density: $1.35{\cdot}10^8$ cells/cm^3 Disk thickness: 1.5 mm Disk diameter: 11 mm Exposed area: 9.35 mm	Collagen	Neonatal rat CMs	7 days of ischemia:Gradient of medium penetration within the disk depth in spinner flask culture (compared to uniform media perfusion through the scaffold)	Cell death Anaerobic metabolism Cell cycle arrest at the G2/M phaseNot uniform cell distribution (cells concentrated at the disk surface) Arrhythmic contraction pattern	(Radisic et al., 2004)
Disk Cell density: $1.5{\cdot}10^8$ cells/cm^3 Disk thickness: 1.8 mm Disk diameter: 3.6 mm	Collagen	Neonatal rat ventricular CMs	16 days of ischemia: Gradient of medium penetration within the disk depth in static culture	Cell death Anaerobic metabolism Total cell number and cell viability decrease from the top construct surface to the bottom construct surface Absence of cardiac markers in bottom cells O_2 linear decrease from the top construct surface to the bottom construct surface	(Radisic et al., 2006)
Disk sandwitched between two plastic disks Cell density: 5, 10 and 15 $\cdot 10^6$ cells/mL Disk diameter: 4, 6 and 7.2 mm	Collagen-Matrigel	Neonatal rat ventricular CMs	0.5, 4, 18 and 36 h of ischemia: Radial gradient of medium penetration within the disk 0, 10, 20, 70 % O_2 Presence of metabolic inhibitors	Hypoxic cells at the disk radial center (diameter of the hypoxic area dependent on cell density, disk diameter, O_2 concentration and presence of metabolic inhibitors)	(Brown et al., 2007)
Ring for mechanical stretching (7 days) to enhance cell functionality Ring inner diameter: 5 mm Ring outer diameter: 10 mm Ring height: 5 mm	Collagen type I -Matrigel (9:1)	Neonatal rat CMs and non-myocytes cells (1:1)	6 h of ischemia: 1 % O_2 12 h of reperfusion: Standard O_2	Downregulation of the cell survival regulators Akt and Bcl-2 Dephosphorylation of gap junctional protein connexin 43 Loss of normal conduction Decrease of I/R effects with preventive pro-survival drug treatment	(Katare et al., 2010)
Ring for mechanical stretching (7 days) to enhance cell functionality	Collagen type I	CMs (60–70 %) and non-myocytes differentiated from hESC	Cryoinjury over the width and one-third of the construct length	Localized cell death Reduction of active contractile force Neonatal response to cryoinjury, without fibrosis or hypertrophy features Regeneration and contractile force recovery after 14 days, dependent on CM proliferation (neonatal features)	(Voges et al., 2017)
8 cardiac spheroids spatially distributed in a ring-shape within the hydrogel	Hyaluronic acid	hiPSC-CMs hCFs	Damage area recreated by 1–2 spheroids with higher proportion of hCF than “healthy” spheroids	Lack of gap-junction formation in damage areas Wave-like propagation of calcium activation Reduced CTD and calcium flux amplitude in damage areas Slower time-to-peak in damaged areas CM proliferation, tissue remodelling and improvement of contractile activity after miRNA treatment	(Mastikhina et al., 2021)
–	De-cellularized extracellular matrix (ECM) from human cardiac samples	hESC-CMs	ECM from ischaemic hearts (*vs* healthy donnors)	Altered contractile activity Non-myocyte population increase Increased expression of α-actinin Reduced troponin organization	(Zhao et al., 2022)

vivo ischemia dependent of other cardiac cells, such as fibrosis. Scaffold-based approaches also fail in mimicking blood flow and capillary-myocardium interfaces, which can improve the recreation of gradients and reperfusion events. Moreover, although mechanical stretching enhances CM functionality, the recreation of an ischaemic event on a mature human myocardium model still remains elusive, maybe requiring combination with other maturation strategies, such as higher cell density to increase cell-to-cell connections, chemical induction of hiPSC-CM maturation, or coculture with other cardiac cells (Karbassi et al., n.d.). In conclusion, similar to spheroid systems, currently developed scaffold-based models of cardiac ischemia do not assess the recreation of combined ischaemic features, like blood reperfusion, adrenergic stimulation, or immune system implication.

4. Heart-on-chip

4.1. Heart-on-chip technologies

The development of microfluidics and microfabrication technologies, in combination with cell culture techniques, opens the door to unprecedented opportunities for the biomimetic recapitulation of human tissue features in vitro, including cardiac tissues. Diverse microdevices have been designed in the last two decades for the simulation of different myocardium particularities, generating a wide range of heart-on-chip models. Cardiac microfluidic platforms can serve for the culture and study of single cells (Kaneko et al., 2007), monolayers (Ugolini et al., 2016), biopsies (Cheah et al., 2010), spheroids (Christoffersson et al., 2018) and scaffold-embedded cells (Veldhuizen et al., 2020), in monoculture or coculture, incorporating CMs, CFs, or endothelial cardiac cells (Veldhuizen et al., 2020; Zhang et al., 2016). Although other in vitro cell culture technologies, like spheroids or scaffolds, already offer the possibility of generating physiological-like 3D constructs and controlled spatial cell distribution, heart-on-chip platforms enable the precise control of many other biochemical and electro-mechanical features of cardiac cell microenvironment.

The implementation of flow systems allows the controlled perfusion of media inside cardiac microdevices, thus recreating outcomes of blood flow, such as capillary-tissue interface, mass transport within the tissue, speed ranges of nutrients supply and waste washout, or shear stress stimulus (Kobuszewska et al., 2017; Ren et al., 2013). Physiological gradients of oxygen, nutrients or drugs can also be simulated in heart-on-chip platforms (Mathur et al., 2015; Ren et al., 2013; Veldhuizen et al., 2020; Zhang et al., 2016). The combination of materials with different mechanical properties and specific designs in microdevice fabrication enables the simulation of mechanical stimulus over the cells. CM monolayers cultured over flexible sheets or 3D constructs anchored to flexible pillars recreate cells passive tension that improves contractile function and CM maturation (Anna Grosberg et al., 2011; Ronaldson-Bouchard et al., 2018). Dynamic cyclic stretching applied to cardiac microtissues with motorized or pneumatic loading systems can also simulate physiological- or disease-like strains, sensed by cardiac cells in vivo (Marsano et al., 2016; Ugolini et al., 2016). Moreover, CMs can be electrically stimulated to mimic myocardium electrophysiology by incorporation of electrodes to heart-on-chip platforms (Marsano et al., 2016). Another advantage of heart-on-chip models is the capacity to monitor several cellular parameters in situ. Microdevices usually present good access to optical microscopic inspection, which allows tracking of fluid patterns and mass transport with fluorescent beads, Ca^{2+} transients (Zhao et al., 2019), or cardiac contraction (Veldhuizen et al., 2020). In fact, along with beating rhythm and amplitude, optical analysis of anchoring pillars deflexion can be used to determine contractile force (Serrao et al., 2012). The implementation of piezoresistive cantilevers, pressure or electrical sensors coupled to carbon nanotubes can also provide quantitative force measurements (Matsudaira et al., 2017; Trzewik et al., 2004; Wang et al., 2018). Electrical activity and action potentials inside heart-on-chip microdevices have also been measured by means of electrical sensors (Liu et al., 2020). Altogether, these heart-on-chip tools offer great opportunities for accurately recreate myocardium microenvironment and get insight of cardiac cellular response to different stimuli.

4.2. Ischaemic heart-on-chip

Precise control and monitoring of oxygen concentration are key for developing in vitro models of cardiac ischaemia. Organ-on-chip technology can overcome the drawbacks from spheroids and cardiac constructs to quantify oxygen within tissues. A simple approach is the optical monitoring overtime of a fluorescent ruthenium-based oxygen-sensitive dye inside a polydimethylsiloxane (PDMS) microfluidic device. The microdevice presents two separated chambers (Fig. 3A), one chamber for 2D culturing of porcine primary CMs and the other containing the dye (Khanal et al., 2011). To avoid shear stress on the cells, a syringe pump pushes cell medium through a microchannel connected laterally to the cell chamber, allowing nutrients to reach cells via low-shear mass transport. The microdevice can be placed inside a polycarbonate box on the microscope stage with nitrogen flowing inside the box to displace oxygen and mimic ischaemia for up to 5 h, followed by 1 h of oxygen restoration, mimicking reperfusion. The oxygen permeability of PDMS ensures no negligible differences on oxygen concentration between the microdevice chambers during the experiment. Dye fluorescence intensity increase correlates with the quick oxygen fall to less than 1 % after 30 min of nitrogen flow, following ischaemia/reperfusion outcomes by porcine CM morphology and viability. After 1 h of ischaemia, almost all cells retract into spherical shape, increasing the apoptotic cell fraction after 2 h of ischaemia, assessed by MitoTracker staining of mitochondria, and confirming the contribution of apoptosis pathway to CMs death burden during ischemia. Although the apoptotic fraction during reperfusion is variable between experiments preventing to stablish a robust conclusion of the effects of oxygen restoration, this first approach to model cardiac ischemia in a heart-on-chip devices opens the door to real-time monitoring of oxygen levels along with cellular markers of cell death pathways for the unravelling of CMs death mechanisms and timing during I/R injury. However, the system does not allow direct oxygen concentration quantification along the cellular chamber and only relies on external application of hypoxia to mimic ischaemia, without investigating possible nutrient gradients within the cellular chamber. 2D culture and porcine cells also reduce the relevance of the model to recreate the features of in vivo human cardiac ischaemia.

The implementation of an oxygen control system in the upstream media reservoir allows the perfusion of accurately defined oxygen concentration media into a heart-on-chip microdevice (Liu et al., 2020). The microdevice, fabricated in PDMS, with immortalized mouse atrial HL-1 cells 2D monolayer in a single channel, is perfused with medium at low flow rates. The upstream media oxygen control enables temporal modulation of oxygen concentration, switched from normoxic (21 %) to hypoxic (1 %), and followed by restoration of normoxia, to simulate I/R changes. This system is used for either acute induction of hypoxia or a gradual switch with an intermediated step of 20 min of 4 % oxygen. As a novelty, extracellular features (beat rates, rhythmicity, and wavefront propagation velocities) are monitored by bioelectronics interface in the microfluidic channel bottom surface (Fig. 3B), with planar electrodes, while intracellular outcomes (shape and duration of action potentials at single-cell level) are determined by arrays of Pt nanopillars that enter into the cellular cytosol, providing insight into spatial heterogeneity of cellular function. Bioelectronic monitoring shows initial tachycardia after hypoxia induction, followed by gradual frequency reduction until arrhythmia, returning to basal rhythm 30 min after oxygen restoration. The high yield of multiplexed readouts enables the generation of isochronal maps for studying wavefront propagation velocity, uniform during normoxia but variable and slower during hypoxia. Intracellular outputs also demonstrate hypoxic-related alterations of action potential, with reduced repolarization and depolarization times. Although

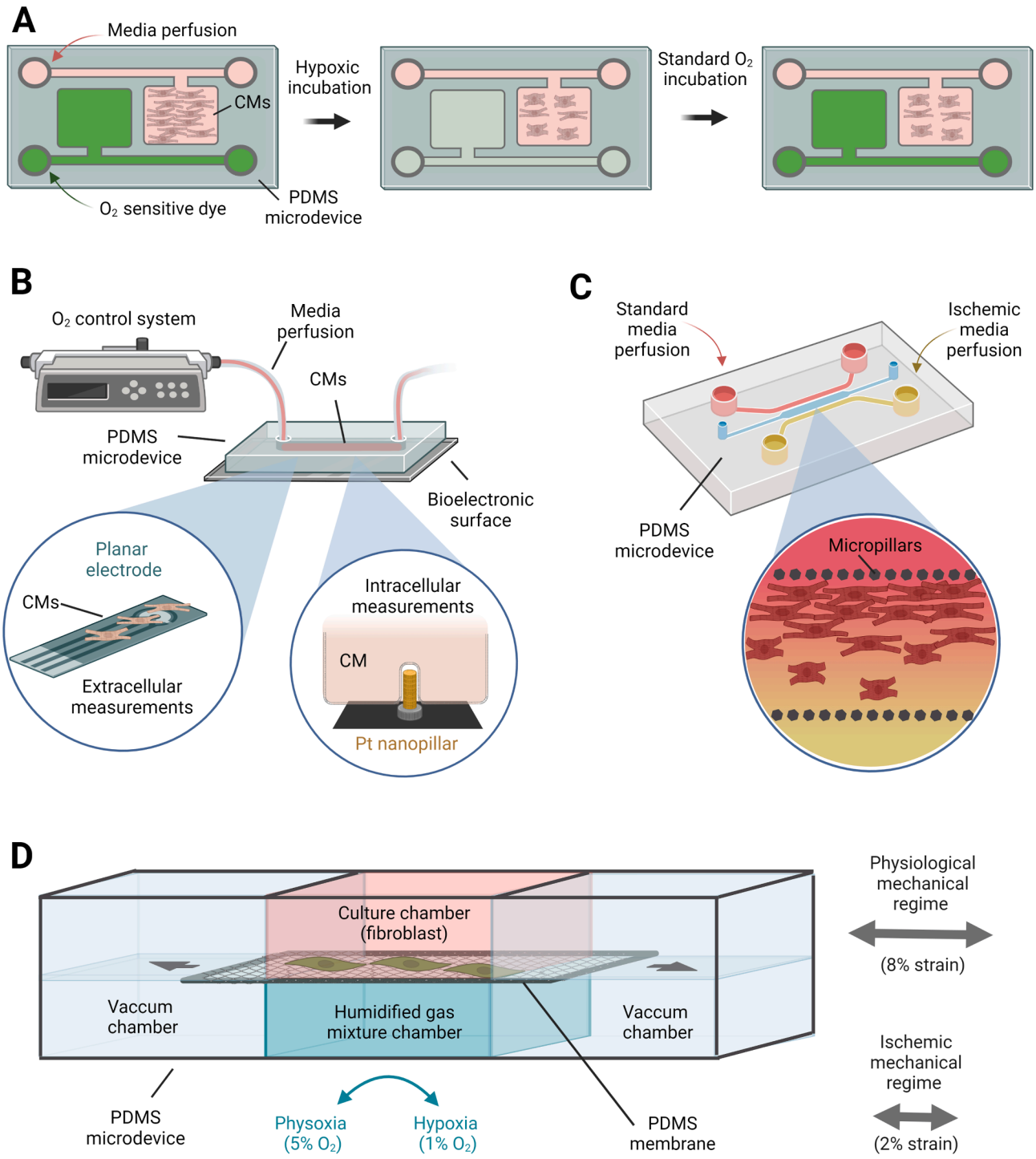

Fig. 3. Ischaemic heart-on-chip models based on 2D cell culture systems. A) O_2 concentration within the gas-permeable PDMS microdevice is determined by quantifying fluorescence from an O_2-sensitive dye. B) Single-channel microdevice with controlled gas composition media perfusion and bottom bioelectronics interface for extracellular and intracellular measurements. C) Arrays of micropillars between the cell culture chamber and lateral channels of a microdevice allow recreation of capillary-tissue interface and molecule gradients. D) Monolayer of cells seeded on flexible membrane are mechanically stimulated by application of vacuum in the adjacent chambers, deforming the membrane, while perfusion of gas with defined composition through the bottom channel allows hypoxia recreation. Created with BioRender.com.

implementation of bioelectronics enhances the analytical power of the model, several aspects of myocardial tissue and in vivo ischaemia are not accurately recapitulated. This 2D culture only relies on uniform oxygen deprivation to recreate ischaemia, without addressing shear stress implications caused by direct flow over the cells, or oxygen concentration alteration inside the microfluidic channel due to the high gas permeability of PDMS. Addressing these issues, along with implementing human cells such as hiPSC-CM and hCF, could increase the accuracy of the model to mimic cardiac ischaemia.

Taking advantage of fluidics to recreate a gradient of oxygen accessibility, monolayers of rat heart H9c2 cells were culture within the central chamber of a PDMS microfluidic device, separated from two lateral channels by symmetrical arrays of micropillars for perfusion with a syringe pump (Ren et al., 2013). The small space left between

micropillars mimics the capillary-myocardium interface, achieving rapid nutrient transport to the central chamber, while maintaining low shear-stress over the cells (Fig. 3C). PDMS gas permeability prevents accurately oxygen changes by media flow modification or blocking. Thus, FCCP, a chemical mitochondrial respiratory chain blocker, recreates the incapacity of cells to incorporate oxygen to their metabolism, added to the use of serum-free medium, mimicking a less nourishing environment. Prior to cell culture and ischaemia induction, nutrient transport and distribution inside the microdevice is assessed by optical monitoring of fluorescein perfused through one channel. A range of symmetrical and non-symmetrical flow rates mimicking capillary blood velocity are tested, obtaining a range of fluorescence gradient inside the central chamber. These gradients can be used to spatially recreate an ischaemic area. Indeed, when culturing cells for 2 h with standard medium perfused in one channel and serum-free medium containing FCCP perfused in the other, cells suffer a shrinkage, lose cell-to-cell contacts, present disrupted actin filaments and show a decrease in their mitochondrial membrane potential. These ischaemic markers are more evident as cells are closer to the "ischaemic" channel, correlating with the increase of caspase-3 positive cell percentage. This model confirms the recreation of an ischaemic gradient by combining hypoxia and medium supplement depletion Fluorescein analysis of mass transport and distribution is a useful tool to determine flow parameters for recreating a physiological or pathological environment inside a microdevice. However, achieving a real quantifiable oxygen reduction inside the chamber, along with nutrient gradient, mainly glucose, would be more representative of the in vivo ischaemia. Culturing cells from human sources in a 3D structure, along with assessing effects of reperfusion, could also increase the predictive power of the model.

The implementation of mechanical stretching with oxygen control and sensors in PDMS microdevices allows mimicking the biochemical and mechanical features of an ischaemic environment (Ugolini et al., 2017). Thus, primary hCFs are cultured on a thin PDMS membrane that can be stretched by means of a vacuum system in two adjacent chambers. A humidified gas mixture with controlled composition is perfused under the culture chamber (Fig. 3D). The PDMS membrane permeability guarantees homogenous gas distribution in the culture chamber, confirmed by an oxygen sensor adjusted with a micromanipulator to reach the culture membrane. Thus, basal oxygen concentration, prior to ischaemic recreation, is settled at 5 %, the physiological concentration in the normal myocardium and henceforward referred as "physoxia", instead of 21 % used in in vitro cultures (henceforward, "normoxia"). A physiological mechanical regime is simulated by applying 8 % strain at 1 Hz stimulus. Ischaemia is recreated within this microdevice by either changing oxygen concentration to 1 % (hypoxia) or reducing mechanical stimulus to 2 % strain. Cellular response is studied under static conditions, 8 % strain and 2 % strain, in combination with either physoxia or hypoxia. Interestingly, hypoxia causes hCFs in static conditions to activate proliferative responses (i.e. YAP nuclear translocation, secretion of mitogenic PDGF, and higher mitotic cell fraction), which is prevented in cells under physiological mechanical 8 % strain. Hypoxia also increases collagen synthesis in both static and 8 % strain conditions. When hCF are only exposed to ischaemic-like mechanical load (2 % strain), with physiological oxygen concentration, they also show proliferative responses, but no collagen increment. However, when both ischaemic stimuli are implemented (2 % mechanical strain and 1 % oxygen), hCF display significant increases in their proliferation, inflammatory activity (production of cytokine IL1-β) and fibrotic remodelling response (secretion of TGF-β and matrix-degrading enzymes MMP-2 and MMP-3). These results demonstrate the importance of recreating the physical environment when modelling myocardial ischaemia. However, myofibroblast differentiation, commonly observable in animal models of myocardial ischaemia (Small et al., 2010) and in in vitro 3D cocultures (Richards et al., 2020b), is not reproduced by this model. A more complex model, that implements cardiomyocytes, 3D structures and ischaemic reduction of nutrients, may help in recreating in vivo cell response to ischaemia.

Combining hiPSC-CMs embedded in collagen-fibrin hydrogels and a PDMS microdevice including two pairs of flexible pillars results in cell alignment and mechanical maturation of the tissue after 2 weeks (Chen, 2018). The construct is subjected to an ischaemia/reperfusion protocol, replacing standard media with an ischaemic solution (saline solution with lactate and pH = 6.4) and placing the microdevice into a hypoxic chamber (95 % N2, 5 % CO_2) for 6 h, followed by reestablishment of control conditions. The model recapitulates well-known damage effects of ischaemia (disruption of CM cytoskeletal fibres, caspase-3 activation and cell death) that are boosted by reperfusion (ROS generation, mitochondrial depolarization, and higher cell death numbers). Notably, when the I/R process is applied to immature constructs (cultured for only 3 days), these effects are highly mitigated, thus demonstrating that cell maturation properly recapitulates the consequences of an ischaemic event in the adult myocardium. Although lacking other cardiac cells implicated in myocardium ischaemic responses, like CF-dependent fibrosis, it is a powerful approach to investigate strategies for CM death prevention or proliferation enhancement. In fact, media acidification, treatment with antioxidants, or use of the mitochondria depolarization-regulator CsA applied during reperfusion results in reduction of cell death markers in the cardiac model.

A similar anchoring pillar-based microdevice coculturing hCFs and hiPSC-CMs can recreate myocardial fibrosis (Mastikhina et al., 2020), a wound healing process leaded by fibroblasts and triggered by cardiac damage events, such as ischaemic injury. Fibrosis results in excessive deposition of extracellular matrix components and tissue stiffness increase, jeopardizing myocardial function. Cells at 3:1 ratio (hiPSC-CM to hCF) are seeded in fibrin gels, facilitating the assessment of cellular deposited collagen, which then led for microtissue compaction and cultured up to 3 weeks. To induce fibrosis, fibroblasts are previously activated by 2D culture in presence of TGF-β1, comparing microtissue biomechanical features to microtissues generated with non-activated fibroblast. Optical monitoring of pillar deflexion allows the determination of microtissue passive (at peak cardiomyocyte relaxation) and contraction force (during peak cardiomyocyte contraction), while atomic force microscopy enables microtissue stiffness characterization. Fibrotic microtissues present lower contraction force, higher passive tension and higher stiffness than control microtissues, correlating with an increase on both interstitial collagen deposition and collagen type I to III ratio in fibrotic microtissues. Moreover, while presence of alpha smooth muscle actin (α-SMA), a marker of myofibroblast activation, is increased on fibrotic tissues; vimentin and cTnT positive cells, as well as proliferation and apoptosis, are similar in fibrotic and control tissues, indicating that the reduction of contractile force in fibrotic tissues is not caused by a potential loss of cardiomyocytes. Interestingly, standard drugs for cardiac failure decrease fibrotic markers more than in 2D culture, demonstrating the high impact of cellular 3D microenvironment on myocardium modelling for drug research. The implementation of an ischaemic protocol (O_2 reduction and nutrient deprivation, possibly combined with other ischaemic cues) could be used to recreate CM damage and ischaemic-dependent CF activation and fibrosis, mimicking key hallmarks of ischaemic disease.

Recently, a new heart-on-chip microdevice that relies on surface topographic patterning, instead of anchoring flexible pillars, to induce 3D cell anisotropic alignment, has been used to simulate I/R myocardial injury (Veldhuizen et al., 2021). hiPSC-CMs and hCFs at 4:1 ratio embedded in collagen-Matrigel hydrogel within a central culture chamber, presenting an array of micropillars around which cells align to, forming an anisotropic 3D structure, are nourished by two lateral channels. After 2 weeks, microdevices are incubated for 24 h in either normoxic (21 % O_2), physioxic (5 % O_2) or hypoxic (1 % O_2) chambers, quantifying oxygen availability inside the microtissue by fluorescent imaging of a reductase activity-based probe. Although oxygen deprivation has no significant effect on cell alignment, hypoxic microtissues show lower synchronicity of cardiac beating, correlating with decreased

expression of calcium-handling and contraction-related genes (ATP2A2 and RYR2) and higher expression of tissue remodelling markers (VEGFA and α-SMA). Whole transcriptomic analysis shows a swift to glycolytic metabolism, enhanced angiogenesis, and downregulation of DNA replication on hypoxic microtissues. Interestingly, viability remains around 88–90 % for hypoxic tissues but significantly falls after oxygen reperfusion, while lactate levels increase during hypoxia and are reduced during reperfusion. Gene expression also trends towards basal levels after oxygen restoration. The data obtained reveals the differential outcomes of ischaemia and reperfusion, and the great potential of the model for drug and cardiac therapeutic research, that includes human fibroblast and achieve CM 3D anisotropic alignment.

The wide variety of biochemical and biomechanical cues implemented in heart ischaemia-on-chip models (Table 3), including 3D coculture, oxygen and nutrient gradients, capillary-tissue interface mimicking, accurate media composition overtime, defined spatial cell distribution, cell anchoring supports, and mechanical stretching, allows precise biomimetic recreation of characteristic features of myocardial tissue and ischaemic injury. Moreover, organ-on-chip technology offers the possibility to accurately monitor several parameters during ischaemia recreation, such as in situ oxygen availability, quantitative CM contractile force or electrical measurements. The combination of these ischaemic cardiac features, along with deep monitoring in a single microdevice is technically challenging, with current models focused on recreating and study few and particular aspects of the in vivo myocardial ischaemia process.

5. Perspectives

In vitro modelling of the human heart has shown an incredibly

Table 3
Heart-on-chips for myocardial ischaemia modelling.

O_2 control system	Stimuli or monitoring system	Medium perfusion	2D/3D culture	Cell types	Ischaemic stimulus	Ischaemic hallmark recreated	Ref.
Optical monitoring of fluorescent ruthenium-based oxygen sensitive dye	–	Through a lateral channel	2D	porcine primary CMs	5 h of ischemia: N_2 replacement of external O_2 1 h of reperfusion: External O_2 restoration	Cell shrinkage Apoptosis	(Khanal et al., 2011)
Oxygen sensor upstream media reservoir	Bioelectronic bottom inferface for extracellular and intracellular measurements	Directly through cell chamber	2D	mouse atrial HL-1 cells	Ischemia: Medium's O_2 reduction to 1 % Reperfusion: Medium's O_2 restoration to 21 %	Action potential alterationsBeating frequency alterations (tachycardia and arrhythmia)	(Liu et al., 2020)
–	–	Through lateral channels separated by micropillar arrays	2D	rat heart H9c2 cells	Ischemia: Perfusion of serum-free medium with FCCP	Gradient of damage Cell shrinkage Loss of cell-to-cell contacts Disrupted actin filaments Apoptosis	(Ren et al., 2013)
Gas of controlled composition perfused under the culture chamber monitored by fine-tip oxygen sensor at cell level	Mechanical stretching	Static culture	2D	human ventricular CF	24 h of ischemia: 1 % O_2Reduced mechanical load (2 % strain)	CF proliferation CF inflammatory activity increase CF fibrotic remodelling response increase	(Ugolini et al., 2017)
	Cell anchoring pillars	Static culture	3D	hiPSC-CM	6 h of ischemia: N_2 replacement of external O_2 Nutrient reduction Reperfusion: Standard conditions restoration	Cell death Apoptosis Cytoskeletal disruption ROS generation and mitochondrial depolarization during reperfusion Reduced effects in immature constructs Reduced effects after different therapeutic strategies	(Chen, 2018)
–	Cell anchoring pillars	Static culture	3D	hiPSC-CM hCF (3:1)	Fibrosis: Use of hCF previously activated with TGF-β1	Low contraction force High passive tension, stiffness, collagen deposition and collagen type I to III ratio	(Mastikhina et al., 2020)
Optical monitoring of a reductase activity-based probe fluorescence	Topographic patterning to induce anisotropic alignment	Static culture	3D	hiPSC-CM hCF (4:1)	24 h of ischemia: 1 % external O_2	High expression of tissue remodelling markers Low expression of calcium-handling and contraction-related genes Beating frequency alterations Anaerobic metabolism Enhanced angiogenesis Low proliferationCell death (during reperfusion)	(Veldhuizen et al., 2021)

blossoming in the last decades thanks to the development of stem cell technologies for obtaining human CM. However, current heart models have not been translated to robust cardiac ischemia modelling yet, with few promising works mimicking myocardial ischemic events in vitro.

One of the major drawbacks of human cardiac ischaemia models' development is the recreation of a mature heart. Assessing physiological features of adult myocardium is fundamental for ischaemia modelling, since ischaemic events are more likely to happen in adult hearts, with lower regenerative potential than their neonatal counterpart (Heallen et al., 2013; Porrello et al., 2013). Neonatal and hiPSC-derived CMs with immature phenotype allow generation of in vitro cardiac microtissues, but require posterior maturation, currently not fully achieved in the lab. Cellular organization in 3D structures, like self-aggregation in spheroids, enhances CM maturation (Correia et al., 2018), especially when co-cultured with other cardiac cells, such as CF (Munawar and Turnbull, 2021), but lack other maturation cues, like mechanical induction of cell anisotropic alignment. The structural support of scaffolds allows implementation of cell anchoring systems and mechanical stretching, inducing cell alignment and maturation. Implementation of elastic membranes for stretching or topographical patterning for alignment induction in heart-on-chip microdevices has also improved CM maturation (Carlos-Oliveira et al., 2021). A combination of strategies, including chemical inductors of maturation, 3D coculture with CF and other cardiac cells, high cell density to favour cell-to-cell connections and mechanical stimulus for cell alignment should be tested to achieve more mature myocardium in vitro. However, even the most advanced reports fail short of their natural counterpart, with the engineered myocardium still comparable to foetal tissue (Ronaldson-Bouchard et al., 2018).

In addition, modelling cardiac ischaemia requires the implementation of a protocol that reproduces the phenomena during an ischaemic event in the human heart. Current models have mimicked CM damage caused by an hypoxic environment, recapitulating the switch towards an anaerobic metabolism, loss of contractile functionality, with changes in calcium-handling and beating rhythm alterations, disruption of sarcomere and cytoskeletal structure, loss of cell-to-cell connections, CM hypertrophy and death (Carrier et al., 2002; Chen and Vunjak-Novakovic, 2019; Richards et al., 2020a). 3D culture in spheroids or scaffolds also allow to recreate O_2 gradients, translated to gradients in CM damage severity (Richards et al., 2020a). Similarly, microfluidic technology mimics blood flow and capillary-tissue interface recreating changes in nutrient composition and O_2 concentration and generating gradients by mass-transport phenomena (Ren et al., 2013). Some works have also recreated the effects of O_2 restoration during reperfusion (Chen and Vunjak-Novakovic, 2019; Sebastião et al., 2020), which causes an increase in ROS and leads to high levels of CM death, recreating fibrotic wound healing process. Co-culturing with CF recreates ischaemic ECM composition changes, tissue remodelling and stiffness increase, also reducing myocardium contractile capacity (Mastikhina et al., 2021; Richards et al., 2020a). Moreover, implementation of mechanical stretching application systems within heart-on-chip microdevices enables mimicking myocardial mechanical load reduction during ischaemia (Ugolini et al., 2017). However, most models focus on the recreation of few features, missing any feedback event and enhancing effects of the combined ischaemic stimuli. As an example, hypoxic environment and reduction of mechanical load cause higher CF activation when combined than separately (Ugolini et al., 2017). Thus, next generation of cardiac ischaemia in vitro models must envision the accurately recreation of the whole complex ischaemic process, from the initial blood flow arrest that leads to gradients of O_2 reduction, nutrient deprivation and end-products accumulation to the effects of reperfusion. Models must also include all cell types implicated in the process triggered by ischaemia, such as tissue remodelling led by CF or inflammatory effects of immune cells, recapitulating paracrine signalling and adrenergic stimulation, along with electromechanical cues (Frangogiannis, 2006).

Modelling the complexity of the myocardial ischaemic injury requires also implementing real-time monitoring of the cardiac response. Cardiac spheroids and organoids fall short in recreating cell alignment, mechanical stimuli and blood flow phenomena; and although they allow bulk experiments, they present limitations for electromechanical characterization measurements and structural imaging by conventional confocal microscopy. Scaffold-based models can overcome some drawbacks, enabling higher control of cellular organization and implementation of both mechanical stimuli and mechanical measurements (Katare et al., 2010; Mastikhina et al., 2020). Finally, culture of spheroids or scaffold-embedded cells within heart-on-chip microdevices may exponentially increase the possibilities for ischaemic stimuli recreation, such as mechanical stimuli and blood flow effects; and implementing real-time monitoring systems, including confocal imaging of microdevices with reduced Z dimension, O_2 spatial measurements, and biosensors for characterization of cardiac cell electrical activity (Liu et al., 2020; Ren et al., 2013; Ugolini et al., 2017).

6. Conclusions

As described, ischaemic cardiac models allow low cost and quick in vitro cultures with human cells. Indeed, combination of in vitro models with CM differentiated from patient hiPSCs may open the door to personalized medicine. Moreover, these novel approaches surpass classical 2D in vitro models by recreating more faithfully myocardial environment, including cellular alignment, coculture of different cardiac cells, mechanical and electrical cues, or blood flow effects, which may enhance their predictive power. In ischaemic heart-on-chip systems, biological, mechanical, and electrical features from myocardial microtissues can be directly monitored in situ, more complex when working with animal models. However, current models cannot fully recreate the complex body reaction to cardiac ischaemia/reperfusion injury (e.g., microvasculature damage or immune inflammation), as animal models do. Novel approaches also fall short in overcoming some of the classical limitations of animal models, such as advanced ages, comorbidities, and severe medication. Finally, alternative treatments assayed in new models should assess not only cell death and infarct size reduction but also attenuation of coronary microvascular obstruction, as well as longer-term targets including infarct repair and reverse remodelling.

In summary, 3D systems, such as spheroids and scaffold-based cardiac constructs, and heart-on-chip models have promisingly recapitulated aspects of myocardial microenvironment and cellular response during cardiac ischaemia. Achieving a highly mature myocardial phenotype and mimicking the variety of ischaemic phenomena within the same model, with further implementation of monitoring techniques, may greatly increase the predictive power of these models for drug research and personalized medicine.

CRediT authorship contribution statement

Laura Paz-Artigas: Conceptualization, Visualization. **Pilar Montero-Calle:** Visualization. **Olalla Iglesias-García:** Visualization. **Manuel M. Mazo:** Visualization, Conceptualization, Writing – review & editing, Supervision, Funding acquisition. **Ignacio Ochoa:** Conceptualization, Supervision, Funding acquisition. **Jesús Ciriza:** Conceptualization, Writing – review & editing, Supervision, Project administration.

Declaration of Competing Interest

The authors declare that they have no known competing financial interests or personal relationships that could have appeared to influence the work reported in this paper.

Data availability

No data was used for the research described in the article.

Acknowledgments

This work has been supported by the European Union's H2020 research and innovation programme under grant agreements No 829010 (PRIME H2020-FETOPEN-2018-2019-2020-01), 778354 (CISTEM H2020-MSCA-RISE-201) and 874827 (BRAV∃); Instituto de Salud Carlos III co-financed by European Regional Development Fund-FEDER "A way to make Europe" PI19/01350. The regional Government of Aragon provided L.P. studentship.

References

Anna Grosberg, W. Alford, P., L. McCain, M., Kit Parker, K., 2011. Ensembles of engineered cardiac tissues for physiological and pharmacological study: Heart on a chip. Lab Chip 11, 4165–4173. https://doi.org/10.1039/C1LC20557A.

Archer, C.R., Sargeant, R., Basak, J., Pilling, J., Barnes, J.R., Pointon, A., 2018. Characterization and Validation of a Human 3D Cardiac Microtissue for the Assessment of Changes in Cardiac Pathology. Sci. Reports 2018 81 8, 1–15. https://doi.org/10.1038/s41598-018-28393-y.

Aurora, A.B., Porrello, E.R., Tan, W., Mahmoud, A.I., Hill, J.A., Bassel-Duby, R., Sadek, H.A., Olson, E.N., 2014. Macrophages are required for neonatal heart regeneration. J. Clin. Invest. 124, 1382–1392. https://doi.org/10.1172/JCI72181.

Basara, G., Saeidi-Javash, M., Ren, X., Bahcecioglu, G., Wyatt, B.C., Anasori, B., Zhang, Y., Zorlutuna, P., 2022. Electrically conductive 3D printed Ti3C2Tx MXene-PEG composite constructs for cardiac tissue engineering. Acta Biomater. 139, 179–189. https://doi.org/10.1016/J.ACTBIO.2020.12.033.

Beauchamp, P., Moritz, W., Kelm, J.M., Ullrich, N.D., Agarkova, I., Anson, B.D., Suter, T. M., Zuppinger, C., 2015. Development and Characterization of a Scaffold-Free 3D Spheroid Model of Induced Pluripotent Stem Cell-Derived Human Cardiomyocytes. Tissue Eng. - Part C Methods. https://doi.org/10.1089/ten.tec.2014.0376.

Bergmann, O., Zdunek, S., Felker, A., Salehpour, M., Alkass, K., Bernard, S., Sjostrom, S. L., Szewczykowska, M., Jackowska, T., Dos Remedios, C., Malm, T., Andrä, M., Jashari, R., Nyengaard, J.R., Possnert, G., Jovinge, S., Druid, H., Frisén, J., 2015. Dynamics of Cell Generation and Turnover in the Human Heart. Cell 161, 1566–1575. https://doi.org/10.1016/J.CELL.2015.05.026.

Brown, D.A., MacLellan, W.R., Laks, H., Dunn, J.C.Y., Wu, B.M., Beygui, R.E., 2007. Analysis of oxygen transport in a diffusion-limited model of engineered heart tissue. Biotechnol. Bioeng. 97, 962–975. https://doi.org/10.1002/BIT.21295.

Buckberg, G.D., 2002. Basic science review: The helix and the heart. J. Thorac. Cardiovasc. Surg. 124, 863–883. https://doi.org/10.1067/mtc.2002.122439.

Buckberg, G.D., Nanda, N.C., Nguyen, C., Kocica, M.J., 2018. What Is the Heart? Anatomy, Function, Pathophysiology, and Misconceptions. J. Cardiovasc. Dev. Dis. 5 https://doi.org/10.3390/jcdd5020033.

Bursac, N., Parker, K.K., Iravanian, S., Tung, L., 2002. Cardiomyocyte Cultures With Controlled Macroscopic Anisotropy. Circ. Res. https://doi.org/10.1161/01.res.0000047530.88338.eb.

Caccioppo, A., Franchin, L., Grosso, A., Angelini, F., D'Ascenzo, F., Brizzi, M.F., 2019. Ischemia Reperfusion Injury: Mechanisms of Damage/Protection and Novel Strategies for Cardiac Recovery/Regeneration. Int. J. Mol. Sci. 20 https://doi.org/10.3390/IJMS20205024.

Carlos-Oliveira, M., Lozano-Juan, F., Occhetta, P., Visone, R., Rasponi, M., 2021. Current strategies of mechanical stimulation for maturation of cardiac microtissues. Biophys. Rev. 13, 717–727. https://doi.org/10.1007/S12551-021-00841-6/FIGURES/4.

Carrier, R.L., Rupnick, M., Langer, R., Schoen, F.J., Freed, L.E., Vunjak-Novakovic, G., 2002. Perfusion improves tissue architecture of engineered cardiac muscle. Tissue Eng. 8, 175–188. https://doi.org/10.1089/107632702753724950.

Cheah, L.T., Dou, Y.H., Seymour, A.M.L., Dyer, C.E., Haswell, S.J., Wadhawan, J.D., Greenman, J., Lih-Tyng Cheah, Yue-Hua Dou, L. Seymour, A.-M., E. Dyer, C., J. Haswell, S., D. Wadhawan, J., John Greenman, Cheah, L.T., Dou, Y.H., Seymour, A. M.L., Dyer, C.E., Haswell, S.J., Wadhawan, J.D., Greenman, J., 2010. Microfluidic perfusion system for maintaining viable heart tissue with real-time electrochemical monitoring of reactive oxygen species. Lab Chip 10, 2720–2726. https://doi.org/10.1039/c004910g.

Chen, Yin, Wang, Junping, Shen, Bo, Y Chan, Camie W, Wang, Chaoyi, Zhao, Yihua, Chan, Ho N, Tian, Qian, Chen, Yangfan, Yao, Chunlei, Hsing, I.-M., Li, Ronald A, Wu, Hongkai, Chen, Y, Yao, C, Hsing, I., Wu, H, Wang, J, Y Chan, C W, Li, R A, Shen, B, Zhao, Y, Chan, H N, Tian, Q, Wang, C, 2015. Engineering a Freestanding Biomimetic Cardiac Patch Using Biodegradable Poly(lactic-co-glycolic acid) (PLGA) and Human Embryonic Stem Cell-derived Ventricular Cardiomyocytes (hESC-VCMs). Macromol. Biosci. 15, 426–436. https://doi.org/10.1002/MABI.201400448.

Chen, T., Vunjak-Novakovic, G., 2019. Human Tissue-Engineered Model of Myocardial Ischemia-Reperfusion Injury. Tissue Eng. Part A 25, 711. https://doi.org/10.1089/TEN.TEA.2018.0212.

Chen, T., 2018. Human Tissue Engineered Model of Myocardial Ischemia-Reperfusion Injury.

Chou, P.-C., Liu, C.-M., Weng, C.-H., Yang, K.-C., Cheng, M.-L., Lin, Y.-C., Yang, R.-B., Shyu, B.-C., Shyue, S.-K., Liu, J.-D., Chen, S.-P., Hsiao, M., Hu, Y.-F., 2022. Fibroblasts Drive Metabolic Reprogramming in Pacemaker Cardiomyocytes. Circ. Res. 131, 6–20. https://doi.org/10.1161/CIRCRESAHA.121.320301.

Christoffersson, J., Meier, F., Kempf, H., Schwanke, K., Coffee, M., Beilmann, M., Zweigerdt, R., Mandenius, C.-F.-F., 2018. A cardiac cell outgrowth assay for evaluating drug compounds using a cardiac spheroid-on-a-chip device. Bioengineering 5, 36. https://doi.org/10.3390/bioengineering5020036.

Correia, C., Koshkin, A., Duarte, P., Hu, D., Carido, M., Sebastião, M.J., Gomes-Alves, P., Elliott, D.A., Domian, I.J., Teixeira, A.P., Alves, P.M., Serra, M., 2018. 3D aggregate culture improves metabolic maturation of human pluripotent stem cell derived cardiomyocytes. Biotechnol. Bioeng. 115, 630–644. https://doi.org/10.1002/bit.26504.

Cristallini, C., Cibrario Rocchietti, E., Accomasso, L., Folino, A., Gallina, C., Muratori, L., Pagliaro, P., Rastaldo, R., Raimondo, S., Saviozzi, S., Sprio, A.E., Gagliardi, M., Barbani, N., Giachino, C., 2014. The effect of bioartificial constructs that mimic myocardial structure and biomechanical properties on stem cell commitment towards cardiac lineage. Biomaterials 35, 92–104. https://doi.org/10.1016/J.BIOMATERIALS.2013.09.058.

Davidson, S.M., Adameová, A., Barile, L., Cabrera-Fuentes, H.A., Lazou, A., Pagliaro, P., Stensløkken, K.O., Garcia-Dorado, D., 2020. Mitochondrial and mitochondrial-independent pathways of myocardial cell death during ischaemia and reperfusion injury. J. Cell. Mol. Med. 24, 3795–3806. https://doi.org/10.1111/JCMM.15127.

Deitch, S., Gao, B.Z., Dean, D., 2012. Effect of Matrix on Cardiomyocyte Viscoelastic Properties in 2D Culture. Mol. Cell. Biomech. 9, 227.

Desroches, B.R., Zhang, P., Choi, B.-R.-R., King, M.E., Maldonado, A.E., Li, W., Rago, A., Liu, G., Nath, N., Hartmann, K.M., Yang, B., Koren, G., Morgan, J.R., Mende, U., 2012. Functional scaffold-free 3-D cardiac microtissues: A novel model for the investigation of heart cells. Am. J. Physiol. - Hear. Circ. Physiol. 302, 2031–2042. https://doi.org/10.1152/ajpheart.00743.2011.

Dunwoodie, S.L., 2009. The role of hypoxia in development of the Mammalian embryo. Dev. Cell 17, 755–773. https://doi.org/10.1016/j.devcel.2009.11.008.

Eghbali, M., Weber, K.T., 1990. Collagen and the myocardium: fibrillar structure, biosynthesis and degradation in relation to hypertrophy and its regression. Mol. Cell. Biochem. 96, 1–14. https://doi.org/10.1007/BF00228448.

Fomovsky, G.M., Thomopoulos, S., Holmes, J.W., 2010. Contribution of extracellular matrix to the mechanical properties of the heart. J. Mol. Cell. Cardiol. 48, 490–496. https://doi.org/10.1016/j.yjmcc.2009.08.003.

Fontana, G., Gershlak, J., Adamski, M., Lee, J.-S., Matsumoto, S., Le, H.u.D., Binder, B., Wirth, J., Gaudette, G., Murphy, W.L., Fontana, G., Lee, J., Gershlak, J., Matsumoto, S., Gaudette, G., Adamski, M., Le, H.D., Binder, B., Wirth, J., Murphy, W.L., 2017. Biofunctionalized Plants as Diverse Biomaterials for Human Cell Culture. Adv. Healthc. Mater. 6, 1601225. https://doi.org/10.1002/ADHM.201601225.

Frangogiannis, N.G., 2006. The Mechanistic Basis of Infarct Healing. Antioxid. Redox Signal. 8, 1907–1939. https://doi.org/10.1089/ars.2006.8.1907.

Frangogiannis, N.G., 2015. Pathophysiology of Myocardial Infarction. Compr. Physiol. 5, 1841–1875. https://doi.org/10.1002/CPHY.C150006.

Frangogiannis, N.G., 2017. The extracellular matrix in myocardial injury, repair, and remodeling. J. Clin. Invest. 127, 1600–1612. https://doi.org/10.1172/JCI87491.

Frantz, S., Hundertmark, M.J., Schulz-Menger, J., Bengel, F.M., Bauersachs, J., 2022. Left ventricular remodelling post-myocardial infarction: pathophysiology, imaging, and novel therapies. Eur. Heart J. 43, 2549–2561. https://doi.org/10.1093/eurheartj/ehac223.

Gaetani, R., Feyen, D.A.M., Verhage, V., Slaats, R., Messina, E., Christman, K.L., Giacomello, A., Doevendans, P.A.F.M., Sluijter, J.P.G., 2015. Epicardial application of cardiac progenitor cells in a 3D-printed gelatin/hyaluronic acid patch preserves cardiac function after myocardial infarction. Biomaterials 61, 339–348. https://doi.org/10.1016/J.BIOMATERIALS.2015.05.005.

Giacomelli, E., Meraviglia, V., Campostrini, G., Cochrane, A., Cao, X., van Helden, R.W. J., Krotenberg Garcia, A., Mircea, M., Kostidis, S., Davis, R.P., van Meer, B.J., Jost, C. R., Koster, A.J., Mei, H., Míguez, D.G., Mulder, A.A., Ledesma-Terrón, M., Pompilio, G., Sala, L., Salvatori, D.C.F., Slieker, R.C., Sommariva, E., de Vries, A.A.F., Giera, M., Semrau, S., Tertoolen, L.G.J., Orlova, V.V., Bellin, M., Mummery, C.L., 2020. Human-iPSC-Derived Cardiac Stromal Cells Enhance Maturation in 3D Cardiac Microtissues and Reveal Non-cardiomyocyte Contributions to Heart Disease. Cell Stem Cell 26, 862–879.e11. https://doi.org/10.1016/j.stem.2020.05.004.

Gogiraju, R., Bochenek, M.L., Schäfer, K., 2019. Angiogenic Endothelial Cell Signaling in Cardiac Hypertrophy and Heart Failure. Front. Cardiovasc. Med. 6, 20. https://doi.org/10.3389/fcvm.2019.00020.

Guyette, J.P., Charest, J.M., Mills, R.W., Jank, B.J., Moser, P.T., Gilpin, S.E., Gershlak, J. R., Okamoto, T., Gonzalez, G., Milan, D.J., Gaudette, G.R., Ott, H.C., 2016. Bioengineering Human Myocardium on Native Extracellular Matrix. Circ. Res. 118, 56–72. https://doi.org/10.1161/CIRCRESAHA.115.306874.

Heallen, T., Morikawa, Y., Leach, J., Tao, G., Willerson, J.T., Johnson, R.L., Martin, J.F., 2013. Hippo signaling impedes adult heart regeneration. Development 140, 4683–4690. https://doi.org/10.1242/DEV.102798.

Heath, D.E., 2019. A Review of Decellularized Extracellular Matrix Biomaterials for Regenerative Engineering Applications. Regen. Eng. Transl. Med. 5, 155–166. https://doi.org/10.1007/S40883-018-0080-0/TABLES/3.

Herron, T.J., Rocha, A.M.D., Campbell, K.F., Ponce-Balbuena, D., Willis, B.C., Guerrero-Serna, G., Liu, Q., Klos, M., Musa, H., Zarzoso, M., Bizy, A., Furness, J., Anumonwo, J., Mironov, S., Jalife, J., 2016. Extracellular Matrix-Mediated Maturation of Human Pluripotent Stem Cell-Derived Cardiac Monolayer Structure and Electrophysiological Function. Circ. Arrhythmia Electrophysiol. 9 https://doi.org/10.1161/CIRCEP.113.003638.

Hodgson, M.J., Knutson, C.C., Momtahan, N., Cook, A.D., 2017. Extracellular Matrix from Whole Porcine Heart Decellularization for Cardiac Tissue Engineering. Methods Mol. Biol. 1577, 95–102. https://doi.org/10.1007/7651_2017_31.

Hulsmans, M., Clauss, S., Xiao, L., Aguirre, A.D., King, K.R., Hanley, A., Hucker, W.J., Wülfers, E.M., Seemann, G., Courties, G., Iwamoto, Y., Sun, Y., Savol, A.J., Sager, H. B., Lavine, K.J., Fishbein, G.A., Capen, D.E., Da Silva, N., Miquerol, L., Wakimoto, H.,

Seidman, C.E., Seidman, J.G., Sadreyev, R.I., Naxerova, K., Mitchell, R.N., Brown, D., Libby, P., Weissleder, R., Swirski, F.K., Kohl, P., Vinegoni, C., Milan, D.J., Ellinor, P. T., Nahrendorf, M., 2017. Macrophages Facilitate Electrical Conduction in the Heart. Cell 169, 510–522.e20. https://doi.org/10.1016/j.cell.2017.03.050.

Inserte, J., Barrabés, J.A., Hernando, V., Garcia-Dorado, D., 2009. Orphan targets for reperfusion injury. Cardiovasc. Res. 83, 169–178. https://doi.org/10.1093/CVR/CVP109.

Jackman, C.P., Carlson, A.L., Bursac, N., 2016. Dynamic culture yields engineered myocardium with near-adult functional output. Biomaterials 111, 66–79. https://doi.org/10.1016/J.BIOMATERIALS.2016.09.024.

Jiang, L., Chen, D., Wang, Z., Zhang, Z., Xia, Y., Xue, H., Liu, Y., 2019. Preparation of an Electrically Conductive Graphene Oxide/Chitosan Scaffold for Cardiac Tissue Engineering. Appl. Biochem. Biotechnol. 188, 952–964. https://doi.org/10.1007/S12010-019-02967-6/FIGURES/5.

Joshi, J., Brennan, D., Beachley, V., Kothapalli, C.R., 2018a. Cardiomyogenic differentiation of human bone marrow-derived mesenchymal stem cell spheroids within electrospun collagen nanofiber mats. J. Biomed. Mater. Res. - Part A. https://doi.org/10.1002/jbm.a.36530.

Joshi, J., Brennan, D., Beachley, V., Kothapalli, C.R., 2018b. Cardiomyogenic differentiation of human bone marrow-derived mesenchymal stem cell spheroids within electrospun collagen nanofiber mats. J. Biomed. Mater. Res. Part A 106, 3303–3312. https://doi.org/10.1002/JBM.A.36530.

Kaneko, T., Kojima, K., Yasuda, K., 2007. An on-chip cardiomyocyte cell network assay for stable drug screening regarding community effect of cell network size. Analyst. https://doi.org/10.1039/b704961g.

Kang, H.M., Lim, J.H., Noh, K.H., Park, D., Cho, H.S., Susztak, K., Jung, C.R., 2019. Effective reconstruction of functional organotypic kidney spheroid for in vitro nephrotoxicity studies. Sci. Reports 2019 91 9, 1–17. https://doi.org/10.1038/s41598-019-53855-2.

Karbassi, E., Fenix, A., Marchiano, S., Muraoka, N., Nakamura, K., Yang, X., Murry, C.E., n.d. Cardiomyocyte maturation: advances in knowledge and implications for regenerative medicine. https://doi.org/10.1038/s41569-019-0331-x.

Katare, R.G., Ando, M., Kakinuma, Y., Sato, T., 2010. Engineered Heart Tissue: A Novel Tool to Study the Ischemic Changes of the Heart In Vitro. PLoS One 5, e9275.

Kelm, J.M., Djonov, V., Hoerstrup, S.P., Guenter, C.I., Ittner, L.M., Greve, F., Hierlemann, A., Sanchez-Bustamante, C.D., Perriard, J.C., Ehler, E., Fussenegger, M., 2006. Tissue-transplant fusion and vascularization of myocardial microtissues and macrotissues implanted into chicken embryos and rats. Tissue Eng. https://doi.org/10.1089/ten.2006.12.2541.

Kelm, J.M., Ehler, E., Nielsen, L.K., Schlatter, S., Perriard, J.-C., Fussenegger, M., 2004. Design of Artificial Myocardial Microtissues. https://home.liebertpub.com/ten 10, 201–214. https://doi.org/10.1089/107632704322791853.

Khanal, G., Chung, K., Solis-Wever, X., Johnson, B., Pappas, D., 2011. Ischemia/reperfusion injury of primary porcine cardiomyocytes in a low-shear microfluidic culture and analysis device. Analyst 136, 3519–3526. https://doi.org/10.1039/C0AN00845A.

Khodabukus, A., Baar, K., 2009. Regulating Fibrinolysis to Engineer Skeletal Muscle from the C2C12 Cell Line. https://home.liebertpub.com/tec 15, 501–511. https://doi.org/10.1089/TEN.TEC.2008.0286.

Kim, T.Y., Kofron, C.M., King, M.E., Markes, A.R., Okundaye, A.O., Qu, Z., Mende, U., Choi, B.R., 2018. Directed fusion of cardiac spheroids into larger heterocellular microtissues enables investigation of cardiac action potential propagation via cardiac fibroblasts. PLoS One. https://doi.org/10.1371/journal.pone.0196714.

Kobuszewska, A., Tomecka, E., Zukowski, K., Jastrzebska, E., Chudy, M., Dybko, A., Renaud, P., Brzozka, Z., 2017. Heart-on-a-Chip: An Investigation of the Influence of Static and Perfusion Conditions on Cardiac (H9C2) Cell Proliferation, Morphology, and Alignment: https://doi.org/10.1177/2472630317705610 22, 536–546. https://doi.org/10.1177/2472630317705610.

LaBarge, W., Mattappally, S., Kannappan, R., Fast, V.G., Pretorius, D., Berry, J.L., Zhang, J., Mattappally, S., Kannappan, R., Fast, V.G., Pretorius, D., Berry, J.L., Zhang, J., Mattappally, S., Kannappan, R., Fast, V.G., Pretorius, D., Berry, J.L., Zhang, J., Mattappally, S., Kannappan, R., Fast, V.G., Pretorius, D., Berry, J.L., Zhang, J., 2019. Maturation of three-dimensional, hiPSC-derived cardiomyocyte spheroids utilizing cyclic, uniaxial stretch and electrical stimulation. PLoS One 14, e0219442.

Laflamme, M.A., Chen, K.Y., Naumova, A.V., Muskheli, V., Fugate, J.A., Dupras, S.K., Reinecke, H., Xu, C., Hassanipour, M., Police, S., O'Sullivan, C., Collins, L., Chen, Y., Minami, E., Gill, E.A., Ueno, S., Yuan, C., Gold, J., Murry, C.E., 2007. Cardiomyocytes derived from human embryonic stem cells in pro-survival factors enhance function of infarcted rat hearts. Nat. Biotechnol. 25, 1015–1024. https://doi.org/10.1038/nbt1327.

Lee, E.J., Kim, D.E., Azeloglu, E.U., Costa, K.D., 2008. Engineered Cardiac Organoid Chambers: Toward a Functional Biological Model Ventricle. https://home.liebertpub.com/tea 14, 215–225. https://doi.org/10.1089/TEA.2007.0351.

Lee, M.-O.-O., Jung, K.B., Jo, S.-J.-J., Hyun, S.-A.-A., Moon, K.-S.-S., Seo, J.-W.-W., Kim, S.-H.-H., Son, M.-Y.-Y., 2019. Modelling cardiac fibrosis using three-dimensional cardiac microtissues derived from human embryonic stem cells. J. Biol. Eng. 13, 1–17. https://doi.org/10.1186/s13036-019-0139-6.

Leedale, J.A., Kyffin, J.A., Harding, A.L., Colley, H.E., Murdoch, C., Sharma, P., Williams, D.P., Webb, S.D., Bearon, R.N., 2020. Multiscale modelling of drug transport and metabolism in liver spheroids. Interface Focus 10. https://doi.org/10.1098/RSFS.2019.0041.

Lewis-Israeli, Y.R., Wasserman, A.H., Gabalski, M.A., Volmert, B.D., Ming, Y., Ball, K.A., Yang, W., Zou, J., Ni, G., Pajares, N., Chatzistavrou, X., Li, W., Zhou, C., Aguirre, A., 2021. Self-assembling human heart organoids for the modeling of cardiac development and congenital heart disease. Nat. Commun. 2021 121 12, 1–16. https://doi.org/10.1038/s41467-021-25329-5.

Li, R.A., Keung, W., Cashman, T.J., Backeris, P.C., Johnson, B.V., Bardot, E.S., Wong, A. O.T., Chan, P.K.W., Chan, C.W.Y., Costa, K.D., 2018. Bioengineering an electro-mechanically functional miniature ventricular heart chamber from human pluripotent stem cells. Biomaterials 163, 116–127. https://doi.org/10.1016/J.BIOMATERIALS.2018.02.024.

Li, H., Liu, C., Bao, M., Liu, W., Nie, Y., Lian, H., Hu, S., 2020. Optimized Langendorff perfusion system for cardiomyocyte isolation in adult mouse heart. J. Cell. Mol. Med. 24, 14619–14625. https://doi.org/10.1111/jcmm.15773.

Liao, J., Xu, B., Zhang, R., Fan, Y., Xie, H., Li, X., 2020. Applications of decellularized materials in tissue engineering: Advantages, drawbacks and current improvements, and future perspectives. J. Mater. Chem. B 8, 10023–10049. https://doi.org/10.1039/D0TB01534B.

Liu, H., Bolonduro, O.A., Hu, N., Ju, J., Rao, A.A., Duffy, B.M., Huang, Z., Black, L.D., Timko, B.P., 2020. Heart-on-a-Chip Model with Integrated Extra- And Intracellular Bioelectronics for Monitoring Cardiac Electrophysiology under Acute Hypoxia. Nano Lett. 20, 2585–2593. https://doi.org/10.1021/ACS.NANOLETT.0C00076/SUPPL_FILE/NL0C00076_SI_002.PDF.

Louch, W.E., Sheehan, K.A., Wolska, B.M., 2011. Methods in cardiomyocyte isolation, culture, and gene transfer. Journal of Molecular and Cellular Cardiology. Academic Press. https://doi.org/10.1016/j.yjmcc.2011.06.012.

MacIver, D.H., Partridge, J.B., Agger, P., Stephenson, R.S., Boukens, B.J.D., Omann, C., Jarvis, J.C., Zhang, H., 2018a. The end of the unique myocardial band: Part II. Clinical and functional considerations. Eur. J. Cardio-thoracic Surg. 53, 120–128. https://doi.org/10.1093/ejcts/ezx335.

MacIver, D.H., Stephenson, R.S., Jensen, B., Agger, P., Sánchez-Quintana, D., Jarvis, J.C., Partridge, J.B., Anderson, R.H., 2018b. The end of the unique myocardial band: Part I. Anatomical considerations. Eur. J. Cardio-thoracic Surg. 53, 112–119. https://doi.org/10.1093/ejcts/ezx290.

MacLeod, K., 2014. An Essential Introduction to Cardiac Electrophysiology. IMPERIAL COLLEGE PRESS. https://doi.org/10.1142/p888.

Maiullari, F., Costantini, M., Milan, M., Pace, V., Chirivì, M., Maiullari, S., Rainer, A., Baci, D., Marei, H.E.S., Seliktar, D., Gargioli, C., Bearzi, C., Rizzi, R., 2018. A multi-cellular 3D bioprinting approach for vascularized heart tissue engineering based on HUVECs and iPSC-derived cardiomyocytes. Sci. Rep. 8 https://doi.org/10.1038/S41598-018-31848-X.

Marsano, A., Conficconi, C., Lemme, M., Occhetta, P., Gaudiello, E., Votta, E., Cerino, G., Redaelli, A., Rasponi, M., Marsano, A., Conficconi, C., Lemme, M., Occhetta, P., Gaudiello, E., Votta, E., Cerino, G., Redaelli, A., Rasponi, M., 2016. Beating heart on a chip: A novel microfluidic platform to generate functional 3D cardiac microtissues. Lab Chip 16, 599–610. https://doi.org/10.1039/c5lc01356a.

Mastikhina, O., Moon, B.U., Williams, K., Hatkar, R., Gustafson, D., Mourad, O., Sun, X., Koo, M., Lam, A.Y.L., Sun, Y., Fish, J.E., Young, E.W.K., Nunes, S.S., 2021. 3D bioprinting of high cell-density heterogeneous tissue models through spheroid fusion within self-healing hydrogels. Nat. Commun. 2021 121 12, 1–13. https://doi.org/10.1038/s41467-021-21029-2.

Mastikhina, O., Moon, B.U., Williams, K., Hatkar, R., Gustafson, D., Mourad, O., Sun, X., Koo, M., Lam, A.Y.L., Sun, Y., Fish, J.E., Young, E.W.K., Nunes, S.S., 2020. Human cardiac fibrosis-on-a-chip model recapitulates disease hallmarks and can serve as a platform for drug testing. Biomaterials 233. https://doi.org/10.1016/J.BIOMATERIALS.2019.119741.

Mathur, A., Loskill, P., Shao, K., Huebsch, N., Hong, S.G., Marcus, S.G., Marks, N., Mandegar, M., Conklin, B.R., Lee, L.P., Healy, K.E., 2015. Human iPSC-based Cardiac Microphysiological System For Drug Screening Applications. Sci. Reports 2015 51 5, 1–7. https://doi.org/10.1038/srep08883.

Matsudaira, K., Takahashi, H., Hirayama-Shoji, K., 2017. MEMS piezoresistive cantilever for the direct measurement of cardiomyocyte contractile force. J. Micromech. Microeng 27, 105005. https://doi.org/10.1088/1361-6439/aa8350.

Matveeva, V.G., Khanova, M.U., Antonova, L.V., Barbarash, L.S., 2020. Fibrin - A promising material for vascular tissue engineering. Vestn. Transplantologii i Iskusstv. Organov 22, 196–208. https://doi.org/10.15825/1995-1191-2020-1-196-208.

Mazo, M., Pelacho, B., Prósper, F., 2010. Stem cell therapy for chronic myocardial infarction. J. Cardiovasc. Transl. Res. 3, 79–88. https://doi.org/10.1007/s12265-009-9159-9.

Mendibil, U., Ruiz-Hernandez, R., Retegi-Carrion, S., Garcia-Urquia, N., Olalde-Graells, B., Abarrategi, A., 2020. Tissue-Specific Decellularization Methods: Rationale and Strategies to Achieve Regenerative Compounds. Int. J. Mol. Sci. 2020, Vol. 21, Page 5447 21, 5447. https://doi.org/10.3390/IJMS21155447.

Munawar, S., Turnbull, I.C., 2021. Cardiac Tissue Engineering: Inclusion of Non-cardiomyocytes for Enhanced Features. Front. Cell Dev. Biol. 9, 988. https://doi.org/10.3389/FCELL.2021.653127/BIBTEX.

Nakagawa, M., Koyanagi, M., Tanabe, K., Takahashi, K., Ichisaka, T., Aoi, T., Okita, K., Mochiduki, Y., Takizawa, N., Yamanaka, S., 2007. Generation of induced pluripotent stem cells without Myc from mouse and human fibroblasts. Nat. Biotechnol. 26, 101–106. https://doi.org/10.1038/nbt1374.

Navaei, A., Saini, H., Christenson, W., Sullivan, R.T., Ros, R., Nikkhah, M., 2016. Gold nanorod-incorporated gelatin-based conductive hydrogels for engineering cardiac tissue constructs. Acta Biomater. 41, 133–146. https://doi.org/10.1016/J.ACTBIO.2016.05.027.

Neely, J.R., Morgan, H.E., 1974. Relationship between carbohydrate and lipid metabolism and the energy balance of heart muscle. Annu. Rev. Physiol. 36, 413–459. https://doi.org/10.1146/annurev.ph.36.030174.002213.

Pagliaro, P., Penna, C., 2015. Redox signalling and cardioprotection: translatability and mechanism. Br. J. Pharmacol. 172, 1974–1995. https://doi.org/10.1111/BPH.12975.

Pavlacky, J., Polak, J., 2020. Technical Feasibility and Physiological Relevance of Hypoxic Cell Culture Models. Front. Endocrinol. Lausanne). 11, 57. https://doi.org/10.3389/fendo.2020.00057.

Pereira, A.H.M., Cardoso, A.C., Franchini, K.G., 2021. Isolation, culture, and immunostaining of neonatal rat ventricular myocytes. STAR Protoc. 2, 100950 https://doi.org/10.1016/j.xpro.2021.100950.

Pinto, A.R., Ilinykh, A., Ivey, M.J., Kuwabara, J.T., D'antoni, M.L., Debuque, R., Chandran, A., Wang, L., Arora, K., Rosenthal, N.A., Tallquist, M.D., 2016. Revisiting Cardiac Cellular Composition. Circ. Res. 118, 400–409. https://doi.org/10.1161/CIRCRESAHA.115.307778.

Polonchuk, L., Chabria, M., Badi, L., Hoflack, J.-C.-C., Figtree, G., Davies, M.J., Gentile, C., 2017. Cardiac spheroids as promising in vitro models to study the human heart microenvironment. Sci. Rep. 7, 1–12. https://doi.org/10.1038/s41598-017-06385-8.

Pomeroy, J.E., Helfer, A., Bursac, N., 2020. Biomaterializing the promise of cardiac tissue engineering. Biotechnol. Adv. 42 https://doi.org/10.1016/j.biotechadv.2019.02.009.

Porrello, E.R., Mahmoud, A.I., Simpson, E., Johnson, B.A., Grinsfelder, D., Canseco, D., Mammen, P.P., Rothermel, B.A., Olson, E.N., Sadek, H.A., 2013. Regulation of neonatal and adult mammalian heart regeneration by the miR-15 family. Proc. Natl. Acad. Sci. U. S. A. 110, 187–192. https://doi.org/10.1073/PNAS.1208863110.

Privat-Maldonado, A., Gorbanev, Y., Dewilde, S., Smits, E., Bogaerts, A., 2018. Reduction of Human Glioblastoma Spheroids Using Cold Atmospheric Plasma: The Combined Effect of Short- and Long-Lived Reactive Species. Cancers 2018, Vol. 10, Page 394 10, 394. https://doi.org/10.3390/CANCERS10110394.

Radisic, M., Yang, L., Boublik, J., Cohen, R.J., Langer, R., Freed, L.E., Vunjak-Novakovic, G., 2004. Medium perfusion enables engineering of compact and contractile cardiac tissue. Am. J. Physiol. - Hear. Circ. Physiol. 286, 507–516. https://doi.org/10.1152/AJPHEART.00171.2003/ASSET/IMAGES/LARGE/H40242846105.JPEG.

Radisic, M., Malda, J., Epping, E., Geng, W., Langer, R., Vunjak-Novakovic, G., 2006. Oxygen gradients correlate with cell density and cell viability in engineered cardiac tissue. Biotechnol. Bioeng. 93, 332–343. https://doi.org/10.1002/BIT.20722.

Raedschelders, K., Ansley, D.M., Chen, D.D.Y., 2012. The cellular and molecular origin of reactive oxygen species generation during myocardial ischemia and reperfusion. Pharmacology and Therapeutics. Pergamon. https://doi.org/10.1016/j.pharmthera.2011.11.004.

Ravichandran, R., Venugopal, J.R., Sundarrajan, S., Mukherjee, S., Sridhar, R., Ramakrishna, S., 2013. Expression of cardiac proteins in neonatal cardiomyocytes on PGS/fibrinogen core/shell substrate for Cardiac tissue engineering. Int. J. Cardiol. 167, 1461–1468. https://doi.org/10.1016/J.IJCARD.2012.04.045.

Ren, L., Liu, W., Wang, Y., Wang, J.C., Tu, Q., Xu, J., Liu, R., Shen, S.F., Wang, J., 2013. Investigation of hypoxia-induced myocardial injury dynamics in a tissue interface mimicking microfluidic device. Anal. Chem. 85, 235–244. https://doi.org/10.1021/AC3025812/SUPPL_FILE/AC3025812_SI_001.PDF.

Richards, D.J., Coyle, R.C., Tan, Y., Jia, J., Wong, K., Toomer, K., Menick, D.R., Mei, Y., 2017. Inspiration from heart development: Biomimetic development of functional human cardiac organoids. Biomaterials 142, 112–123. https://doi.org/10.1016/J.BIOMATERIALS.2017.07.021.

Richards, D.J., Li, Y., Kerr, C.M., Yao, J., Beeson, G.C., Coyle, R.C., Chen, X., Jia, J., Damon, B., Wilson, R., Starr Hazard, E., Hardiman, G., Menick, D.R., Beeson, C.C., Yao, H., Ye, T., Mei, Y., 2020a. Human cardiac organoids for the modelling of myocardial infarction and drug cardiotoxicity. Nat. Biomed. Eng. 2020 44 4, 446–462. https://doi.org/10.1038/s41551-020-0539-4.

Richards, D.J., Li, Y., Kerr, C.M., Yao, J., Beeson, G.C., Coyle, R.C., Chen, X., Jia, J., Damon, B., Wilson, R., Starr Hazard, E., Hardiman, G., Menick, D.R., Beeson, C.C., Yao, H., Ye, T., Mei, Y., Hazard, E.S., Hardiman, G., Menick, D.R., Beeson, C.C., Yao, H., Ye, T., Mei, Y., 2020. Human cardiac organoids for the modelling of myocardial infarction and drug cardiotoxicity. Nat. Biomed. Eng. 4, 446–462. https://doi.org/10.1038/s41551-020-0539-4.

Ronaldson-Bouchard, K., Ma, S.P., Yeager, K., Chen, T., Song, L.J., Sirabella, D., Morikawa, K., Teles, D., Yazawa, M., Vunjak-Novakovic, G., 2018. Advanced maturation of human cardiac tissue grown from pluripotent stem cells. Nat. 2018 5567700 556, 239–243. https://doi.org/10.1038/s41586-018-0016-3.

Roth, G.A., Mensah, G.A., Johnson, C.O., Addolorato, G., Ammirati, E., Baddour, L.M., Barengo, N.C., Beaton, A., Benjamin, E.J., Benziger, C.P., Bonny, A., Brauer, M., Brodmann, M., Cahill, T.J., Carapetis, J.R., Catapano, A.L., Chugh, S., Cooper, L.T., Coresh, J., Criqui, M.H., DeCleene, N.K., Eagle, K.A., Emmons-Bell, S., Feigin, V.L., Fernández-Sola, J., Fowkes, F.G.R., Gakidou, E., Grundy, S.M., He, F.J., Howard, G., Hu, F., Inker, L., Karthikeyan, G., Kassebaum, N.J., Koroshetz, W.J., Lavie, C., Lloyd-Jones, D., Lu, H.S., Mirijello, A., Misganaw, A.T., Mokdad, A.H., Moran, A.E., Muntner, P., Narula, J., Neal, B., Ntsekhe, M., Oliveira, G.M.M., Otto, C.M., Owolabi, M.O., Pratt, M., Rajagopalan, S., Reitsma, M.B., Ribeiro, A.L.P., Rigotti, N.A., Rodgers, A., Sable, C.A., Shakil, S.S., Sliwa, K., Stark, B.A., Sundström, J., Timpel, P., Tleyjeh, I.I., Valgimigli, M., Vos, T., Whelton, P.K., Yacoub, M., Zuhlke, L.J., Abbasi-Kangevari, M., Abdi, A., Abedi, A., Aboyans, V., Abrha, W.A., Abu-Gharbieh, E., Abushouk, A.I., Acharya, D., Adair, T., Adebayo, O.M., Ademi, Z., Advani, S.M., Afshari, K., Afshin, A., Agarwal, G., Agasthi, P., Ahmad, S., Ahmadi, S., Ahmed, M.B., Aji, B., Akalu, Y., Akande-Sholabi, W., Aklilu, A., Akunna, C.J., Alahdab, F., Al-Eyadhy, A., Alhabib, K.F., Alif, S.M., Alipour, V., Aljunid, S.M., Alla, F., Almasi-Hashiani, A., Almustanyir, S., Al-Raddadi, R.M., Amegah, A.K., Amini, S., Aminorroaya, A., Amu, H., Amugsi, D.A., Ancuceanu, R., Anderlini, D., Andrei, T., Andrei, C.L., Ansari-Moghaddam, A., Anteneh, Z.A., Antonazzo, I.C., Antony, B., Anwer, R., Appiah, L.T., Arabloo, J., Ärnlöv, J., Artanti, K.D., Ataro, Z., Ausloos, M., Avila-Burgos, L., Awan, A.T., Awoke, M.A., Ayele, H.T., Ayza, M.A., Azari, S., Darshan, B.B., Baheiraei, N., Baig, A.A., Bakhtiari, A., Banach, M., Banik, P.C., Baptista, E.A., Barboza, M.A., Barua, L., Basu, S., Bedi, N., Béjot, Y., Bennett, D.A., Bensenor, I.M., Berman, A.E., Bezabih, Y.M., Bhagavathula, A.S., Bhaskar, S., Bhattacharyya, K., Bijani, A., Bikbov, B., Birhanu, M.M., Boloor, A., Brant, L.C., Brenner, H., Briko, N.I., Butt, Z.A., dos Santos, F.L.C., Cahill, L.E., Cahuana-Hurtado, L., Cámera, L.A., Campos-Nonato, I.R., Cantu-Brito, C., Car, J., Carrero, J.J., Carvalho, F., Castañeda-Orjuela, C.A., Catalá-López, F., Cerin, E., Charan, J., Chattu, V.K., Chen, S., Chin, K.L., Choi, J.Y.J., Chu, D.T., Chung, S.C., Cirillo, M., Coffey, S., Conti, S., Costa, V.M., Cundiff, D.K., Dadras, O., Dagnew, B., Dai, X., Damasceno, A. A.M., Dandona, L., Dandona, R., Davletov, K., de la Cruz-Góngora, V., de la Hoz, F. P., de Neve, J.W., Denova-Gutiérrez, E., Molla, M.D., Derseh, B.T., Desai, R., Deuschl, G., Dharmaratne, S.D., Dhimal, M., Dhungana, R.R., Dianatinasab, M., Diaz, D., Djalalinia, S., Dokova, K., Douiri, A., Duncan, B.B., Duraes, A.R., Eagan, A.W., Ebtehaj, S., Eftekhari, A., Eftekharzadeh, S., Ekholuenetale, M., El Nahas, N., Elgendy, I.Y., Elhadi, M., El-Jaafary, S.I., Esteghamati, S., Etisso, A.E., Eyawo, O., Fadhil, I., Faraon, E.J.A., Faris, P.S., Farwati, M., Farzadfar, F., Fernandes, E., Prendes, C.F., Ferrara, P., Filip, I., Fischer, F., Flood, D., Fukumoto, T., Gad, M.M., Gaidhane, S., Ganji, M., Garg, J., Gebre, A.K., Gebregiorgis, B.G., Gebregzabiher, K. Z., Gebremeskel, G.G., Getacher, L., Obsa, A.G., Ghajar, A., Ghashghaee, A., Ghith, N., Giampaoli, S., Gilani, S.A., Gill, P.S., Gillum, R.F., Glushkova, E. V., Gnedovskaya, E. V., Golechha, M., Gonfa, K.B., Goudarzian, A.H., Goulart, A.C., Guadamuz, J.S., Guha, A., Guo, Y., Gupta, R., Hachinski, V., Hafezi-Nejad, N., Haile, T.G., Hamadeh, R.R., Hamidi, S., Hankey, G.J., Hargono, A., Hartono, R.K., Hashemian, M., Hashi, A., Hassan, S., Hassen, H.Y., Havmoeller, R.J., Hay, S.I., Hayat, K., Heidari, G., Herteliu, C., Holla, R., Hosseini, M., Hosseinzadeh, M., Hostiuc, M., Hostiuc, S., Househ, M., Huang, J., Humayun, A., Iavicoli, I., Ibeneme, C.U., Ibitoye, S.E., Ilesanmi, O.S., Ilic, I.M., Ilic, M.D., Iqbal, U., Irvani, S.S.N., Islam, S.M.S., Islam, R.M., Iso, H., Iwagami, M., Jain, V., Javaheri, T., Jayapal, S.K., Jayaram, S., Jayawardena, R., Jeemon, P., Jha, R.P., Jonas, J.B., Jonnagaddala, J., Joukar, F., Jozwiak, J.J., Jürisson, M., Kabir, A., Kahlon, T., Kalani, R., Kalhor, R., Kamath, A., Kamel, I., Kandel, H., Kandel, A., Karch, A., Kasa, A.S., Katoto, P.D.M.C., Kayode, G.A., Khader, Y.S., Khammarnia, M., Khan, M.S., Khan, M.N., Khan, M., Khan, E.A., Khatab, K., Kibria, G.M.A., Kim, Y.J., Kim, G.R., Kimokoti, R.W., Kisa, S., Kisa, A., Kivimäki, M., Kolte, D., Koolivand, A., Korshunov, V.A., Laxminarayana, S. L.K., Koyanagi, A., Krishan, K., Krishnamoorthy, V., Defo, B.K., Bicer, B.K., Kulkarni, V., Kumar, G.A., Kumar, N., Kurmi, O.P., Kusuma, D., Kwan, G.F., la Vecchia, C., Lacey, B., Lallukka, T., Lan, Q., Lasrado, S., Lassi, Z.S., Lauriola, P., Lawrence, W.R., Laxmaiah, A., LeGrand, K.E., Li, M.C., Li, B., Li, S., Lim, S.S., Lim, L.L., Lin, H., Lin, Z., Lin, R.T., Liu, X., Lopez, A.D., Lorkowski, S., Lotufo, P.A., Lugo, A., Nirmal, K.M., Madotto, F., Mahmoudi, M., Majeed, A., Malekzadeh, R., Malik, A.A., Mamun, A.A., Manafi, N., Mansournia, M.A., Mantovani, L.G., Martini, S., Mathur, M.R., Mazzaglia, G., Mehata, S., Mehndiratta, M.M., Meier, T., Menezes, R.G., Meretoja, A., Mestrovic, T., Miazgowski, B., Miazgowski, T., Michalek, I.M., Miller, T.R., Mirrakhimov, E.M., Mirzaei, H., Moazen, B., Moghadaszadeh, M., Mohammad, Y., Mohammad, D.K., Mohammed, S., Mohammed, M.A., Mokhayeri, Y., Molokhia, M., Montasir, A.A., Moradi, G., Moradzadeh, R., Moraga, P., Morawska, L., Velásquez, I. M., Morze, J., Mubarik, S., Muruet, W., Musa, K.I., Nagarajan, A.J., Nalini, M., Nangia, V., Naqvi, A.A., Swamy, S.N., Nascimento, B.R., Nayak, V.C., Nazari, J., Nazarzadeh, M., Negoi, R.I., Kandel, S.N., Nguyen, H.L.T., Nixon, M.R., Norrving, B., Noubiap, J.J., Nouthe, B.E., Nowak, C., Odukoya, O.O., Ogbo, F.A., Olagunju, A.T., Orru, H., Ortiz, A., Ostroff, S.M., Padubidri, J.R., Palladino, R., Pana, A., Panda-Jonas, S., Parekh, U., Park, E.C., Parvizi, M., Kan, F.P., Patel, U.K., Pathak, M., Paudel, R., Pepito, V.C.F., Perianayagam, A., Perico, N., Pham, H.Q., Pilgrim, T., Piradov, M.A., Pishgar, F., Podder, V., Polibin, R. V., Pourshams, A., Pribadi, D.R.A., Rabiee, N., Rabiee, M., Radfar, A., Rafiei, A., Rahim, F., Rahimi-Movaghar, V., Rahman, M.H.U., Rahman, M.A., Rahmani, A.M., Rakovac, I., Ram, P., Ramalingam, S., Rana, J., Ranasinghe, P., Rao, S.J., Rathi, P., Rawal, L., Rawasia, W.F., Rawassizadeh, R., Remuzzi, G., Renzaho, A.M.N., Rezapour, A., Riahi, S.M., Roberts-Thomson, R.L., Roever, L., Rohloff, P., Romoli, M., Roshandel, G., Rwegerera, G.M., Saadatagah, S., Saber-Ayad, M.M., Sabour, S., Sacco, S., Sadeghi, M., Moghaddam, S. S., Safari, S., Sahebkar, A., Salehi, S., Salimzadeh, H., Samaei, M., Samy, A.M., Santos, I.S., Santric-Milicevic, M.M., Sarrafzadegan, N., Sarveazad, A., Sathish, T., Sawhney, M., Saylan, M., Schmidt, M.I., Schutte, A.E., Senthilkumaran, S., Sepanlou, S.G., Sha, F., Shahabi, S., Shahid, I., Shaikh, M.A., Shamali, M., Shamsizadeh, M., Shawon, M.S.R., Sheikh, A., Shigematsu, M., Shin, M.J., Shin, J. Il, Shiri, R., Shiue, I., Shuval, K., Siabani, S., Siddiqi, T.J., Silva, D.A.S., Singh, J.A., Singh, A., Skryabin, V. Y., Skryabina, A.A., Soheili, A., Spurlock, E.E., Stockfelt, L., Stortecky, S., Stranges, S., Abdulkader, R.S., Tadbiri, H., Tadesse, E.G., Tadesse, D.B., Tajdini, M., Tariqujjaman, M., Teklehaimanot, B.F., Temsah, M.H., Tesema, A.K., Thakur, B., Thankappan, K.R., Thapar, R., Thrift, A.G., Timalsina, B., Tonelli, M., Touvier, M., Tovani-Palone, M.R., Tripathi, A., Tripathy, J.P., Truelsen, T.C., Tsegay, G.M., Tsegaye, G.W., Tsilimparis, N., Tusa, B.S., Tyrovolas, S., Umapathi, K.K., Unim, B., Unnikrishnan, B., Usman, M.S., Vaduganathan, M., Valdez, P.R., Vasankari, T.J., Velazquez, D.Z., Venketasubramanian, N., Vu, G.T., Vujcic, I.S., Waheed, Y., Wang, Y., Wang, F., Wei, J., Weintraub, R.G., Weldemariam, A.H., Westerman, R., Winkler, A.S., Wiysonge, C.S., Wolfe, C.D.A., Wubishet, B.L., Xu, G., Yadollahpour, A., Yamagishi, K., Yan, L.L., Yandrapalli, S., Yano, Y., Yatsuya, H., Yeheyis, T.Y., Yeshaw, Y., Yilgwan, C.S., Yonemoto, N., Yu, C., Yusefzadeh, H., Zachariah, G., Zaman, S. Bin, Zaman, M.S., Zamanian, M., Zand, R., Zandifar, A., Zarghi, A., Zastrozhin, M.S., Zastrozhina, A., Zhang, Z.J., Zhang, Y., Zhang, W., Zhong, C., Zou, Z., Zuniga, Y.M.H., Murray, C.J.L., Fuster, V., 2020. Global Burden of Cardiovascular Diseases and Risk Factors, 1990-2019: Update From the GBD 2019 Study. J. Am. Coll. Cardiol. 76, 2982–3021. https://doi.org/10.1016/j.jacc.2020.11.010.

Ruan, J.L., Tulloch, N.L., Razumova, M.V., Saiget, M., Muskheli, V., Pabon, L., Reinecke, H., Regnier, M., Murry, C.E., 2016. Mechanical Stress Conditioning and Electrical Stimulation Promote Contractility and Force Maturation of Induced Pluripotent Stem Cell-Derived Human Cardiac Tissue. Circulation 134, 1557–1567. https://doi.org/10.1161/CIRCULATIONAHA.114.014998.

Ruiz-Villalba, A., Romero, J.P., Hernández, S.C., Vilas-Zornoza, A., Fortelny, N., Castro-Labrador, L., San Martin-Uriz, P., Lorenzo-Vivas, E., García-Olloqui, P., Palacio, M., Gavira, J.J., Bastarrika, G., Janssens, S., Wu, M., Iglesias, E., Abizanda, G., de Morentin, X.M., Lasaga, M., Planell, N., Bock, C., Alignani, D., Medal, G., Prudovsky, I., Jin, Y.R., Ryzhov, S., Yin, H., Pelacho, B., Gomez-Cabrero, D., Lindner, V., Lara-Astiaso, D., Prósper, F., 2020. Single-Cell RNA Sequencing Analysis Reveals a Crucial Role for CTHRC1 (Collagen Triple Helix Repeat Containing 1) Cardiac Fibroblasts After Myocardial Infarction. Circulation. https://doi.org/10.1161/CIRCULATIONAHA.119.044557.

Saludas, L., Pascual-Gil, S., Prósper, F., Garbayo, E., Blanco-Prieto, M., 2017. Hydrogel based approaches for cardiac tissue engineering. Int. J. Pharm. 523, 454–475. https://doi.org/10.1016/J.IJPHARM.2016.10.061.

Sebastião, M.J., Gomes-Alves, P., Reis, I., Sanchez, B., Palacios, I., Serra, M., Alves, P.M., 2020. Bioreactor-based 3D human myocardial ischemia/reperfusion in vitro model: a novel tool to unveil key paracrine factors upon acute myocardial infarction. Transl. Res. 215, 57–74. https://doi.org/10.1016/j.trsl.2019.09.001.

Segers, V.F.M., Brutsaert, D.L., De Keulenaer, G.W., 2018. Cardiac Remodeling: Endothelial Cells Have More to Say Than Just NO. Front. Physiol. 9, 382. https://doi.org/10.3389/fphys.2018.00382.

Serrao, G.W., Turnbull, I.C., Ancukiewicz, D., Kim, D.E., Kao, E., Cashman, T.J., Hadri, L., Hajjar, R.J., Costa, K.D., 2012. Myocyte-Depleted Engineered Cardiac Tissues Support Therapeutic Potential of Mesenchymal Stem Cells. https://home.liebertpub.com/tea 18, 1322–1333. https://doi.org/10.1089/TEN.TEA.2011.0278.

Sheehy, S.P., Grosberg, A., Qin, P., Behm, D.J., Ferrier, J.P., Eagleson, M.A., Nesmith, A. P., Krull, D., Falls, J.G., Campbell, P.H., McCain, M.L., Willette, R.N., Hu, E., Parker, K.K., 2017. Toward improved myocardial maturity in an organ-on-chip platform with immature cardiac myocytes. Exp. Biol. Med. (Maywood) 242, 1643–1656. https://doi.org/10.1177/1535370217701006.

Small, E.M., Thatcher, J.E., Sutherland, L.B., Kinoshita, H., Gerard, R.D., Richardson, J. A., Dimaio, J.M., Sadek, H., Kuwahara, K., Olson, E.N., 2010. Myocardin-related transcription factor-a controls myofibroblast activation and fibrosis in response to myocardial infarction. Circ. Res. 107, 294–304. https://doi.org/10.1161/CIRCRESAHA.110.223172.

Stevens, K.R., Kreutziger, K.L., Dupras, S.K., Korte, F.S., Regnier, M., Muskheli, V., Nourse, M.B., Bendixen, K., Reinecke, H., Murry, C.E., 2009. Physiological function and transplantation of scaffold-free and vascularized human cardiac muscle tissue. Proc. Natl. Acad. Sci. U. S. A. 106, 16568–16573. https://doi.org/10.1073/pnas.0908381106.

Tallquist, M.D., Molkentin, J.D., 2017. Redefining the identity of cardiac fibroblasts. Nat. Rev. Cardiol. 14, 484–491. https://doi.org/10.1038/nrcardio.2017.57.

Tan, Y., Richards, D., Xu, R., Stewart-Clark, S., Mani, S.K., Borg, T.K., Menick, D.R., Tian, B., Mei, Y., 2015. Silicon nanowire-induced maturation of cardiomyocytes derived from human induced pluripotent stem cells. Nano Lett. 15, 2765–2772. https://doi.org/10.1021/nl502227a.

Thomson, J.A., Itskovitz-Eldor, J., Shapiro, S.S., Waknitz, M.A., Swiergiel, J.J., Marshall, V.S., Jones, J.M., 1998. Embryonic Stem Cell Lines Derived from Human Blastocysts. Science (80-.). 282, 1145–1147. https://doi.org/10.1126/science.282.5391.1145.

Trzewik, J., Artmann-Temiz, A., Linder, P.T., Demirci, T., Digel, I., Artmann, G.M., 2004. Evaluation of Lateral Mechanical Tension in Thin-Film Tissue Constructs. Ann. Biomed. Eng. 32, 1243–1251.

Ugolini, G.S., Rasponi, M., Pavesi, A., Santoro, R., Kamm, R., Fiore, G.B., Pesce, M., Soncini, M., 2016. On-chip assessment of human primary cardiac fibroblasts proliferative responses to uniaxial cyclic mechanical strain. Biotechnol. Bioeng. 113, 859–869. https://doi.org/10.1002/BIT.25847.

Ugolini, G.S., Pavesi, A., Rasponi, M., Fiore, G.B., Kamm, R., Soncini, M., 2017. Human cardiac fibroblasts adaptive responses to controlled combined mechanical strain and oxygen changes in vitro. Elife 6. https://doi.org/10.7554/ELIFE.22847.

Veldhuizen, J., Cutts, J., Brafman, D.A., Migrino, R.Q., Nikkhah, M., 2020. Engineering anisotropic human stem cell-derived three-dimensional cardiac tissue on-a-chip. Biomaterials 256, 120195. https://doi.org/10.1016/J.BIOMATERIALS.2020.120195.

Veldhuizen, J., Chavan, R., Moghadas, B., Park, J.G., Kodibagkar, V.D., Migrino, R.Q., Nikkhah, M., 2021. Cardiac ischemia on-a-chip to investigate cellular and molecular response of myocardial tissue under hypoxia. Biomaterials 121336. https://doi.org/10.1016/J.BIOMATERIALS.2021.121336.

Voges, H.K., Mills, R.J., Elliott, D.A., Parton, R.G., Porrello, E.R., Hudson, J.E., 2017. Development of a human cardiac organoid injury model reveals innate regenerative potential. Dev. 144, 1118–1127. https://doi.org/10.1242/DEV.143966/264220/AM/DEVELOPMENT-OF-A-HUMAN-CARDIAC-ORGANOID-INJURY.

von Bibra, C., Shibamiya, A., Geertz, B., Querdel, E., Köhne, M., Stüdemann, T., Starbatty, J., Schmidt, F.N., Hansen, A., Hiebl, B., Eschenhagen, T., Weinberger, F., 2022. Human engineered heart tissue transplantation in a guinea pig chronic injury model. J. Mol. Cell. Cardiol. 166, 1–10. https://doi.org/10.1016/j.yjmcc.2022.01.007.

Wang, L., Dou, W., Malhi, M., Zhu, M., Liu, H., Plakhotnik, J., Xu, Z., Zhao, Q., Chen, J., Chen, S., Hamilton, R., Simmons, C.A., Maynes, J.T., Sun, Y., 2018. Microdevice Platform for Continuous Measurement of Contractility, Beating Rate, and Beating Rhythm of Human-Induced Pluripotent Stem Cell-Cardiomyocytes inside a Controlled Incubator Environment. ACS Appl. Mater. Interfaces 10, 21173–21183. https://doi.org/10.1021/acsami.8b05407.

Wang, P.Y., Yu, J., Lin, J.H., Tsai, W.B., 2011. Modulation of alignment, elongation and contraction of cardiomyocytes through a combination of nanotopography and rigidity of substrates. Acta Biomater. 7, 3285–3293. https://doi.org/10.1016/j.actbio.2011.05.021.

Yang, B., Lui, C., Yeung, E., Matsushita, H., Jeyaram, A., Pitaktong, I., Inoue, T., Mohamed, Z., Ong, C.S., Disilvestre, D., Jay, S.M., Tung, L., Tomaselli, G., Ma, C., Hibino, N., 2019. A Net Mold-Based Method of Biomaterial-Free Three-Dimensional Cardiac Tissue Creation. Tissue Eng. - Part C Methods. https://doi.org/10.1089/ten.tec.2019.0003.

Yu, J., Vodyanik, M.A., Smuga-Otto, K., Antosiewicz-Bourget, J., Frane, J.L., Tian, S., Nie, J., Jonsdottir, G.A., Ruotti, V., Stewart, R., Slukvin, I.I., Thomson, J.A., 2007. Induced pluripotent stem cell lines derived from human somatic cells. Science (80-.). https://doi.org/10.1126/science.1151526.

Zhang, Y.S., Arneri, A., Bersini, S., Shin, S.-R., Zhu, K., Goli-Malekabadi, Z., Aleman, J., Colosi, C., Busignani, F., Dell'erba, V., Bishop, C., Shupe, T., Demarchi, D., Moretti, M., Rasponi, M., Dokmeci, R., Atala, A., Khademhosseini, Ali, Khademhosseini, A, 2016. Bioprinting 3D microfibrous scaffolds for engineering endothelialized myocardium and heart-on-a-chip. https://doi.org/10.1016/j.biomaterials.2016.09.003.

Zhang, W., Kong, C.W., Tong, M.H., Chooi, W.H., Huang, N., Li, R.A., Chan, B.P., 2017. Maturation of human embryonic stem cell-derived cardiomyocytes (hESC-CMs) in 3D collagen matrix: Effects of niche cell supplementation and mechanical stimulation. Acta Biomater. 49, 204–217. https://doi.org/10.1016/J.ACTBIO.2016.11.058.

Zhao, Y., Rafatian, N., Feric, N.T., Cox, B.J., Aschar-Sobbi, R., Wang, E.Y., Aggarwal, P., Zhang, B., Conant, G., Ronaldson-Bouchard, K., Pahnke, A., Protze, S., Lee, J.H., Davenport Huyer, L., Jekic, D., Wickeler, A., Naguib, H.E., Keller, G.M., Vunjak-Novakovic, G., Broeckel, U., Backx, P.H., Radisic, M., 2019. A Platform for Generation of Chamber-Specific Cardiac Tissues and Disease Modeling. Cell 176, 913-927.e18. https://doi.org/10.1016/J.CELL.2018.11.042.

Zhao, Y., Godier-Furnemont, A., Bax, N.A.M., Bouten, C.V.C., Brown, L.M., Fine, B., Vunjak-Novakovic, G., 2022. Changes in extracellular matrix in failing human non-ischemic and ischemic hearts with mechanical unloading. J. Mol. Cell. Cardiol. 166, 137–151. https://doi.org/10.1016/j.yjmcc.2022.02.003.

Zhao, G., Zhang, X., Lu, T.J., Xu, F., 2015. Recent Advances in Electrospun Nanofibrous Scaffolds for Cardiac Tissue Engineering. Adv. Funct. Mater. 25, 5726–5738. https://doi.org/10.1002/ADFM.201502142.

Zwi, L., Caspi, O., Arbel, G., Huber, I., Gepstein, A., Park, I.H., Gepstein, L., 2009. Cardiomyocyte differentiation of human induced pluripotent stem cells. Circulation 120, 1513–1523. https://doi.org/10.1161/CIRCULATIONAHA.109.868885.